Available online at www.sciencedirect.com

ScienceDirect

J. Differential Equations ••• (••••) •••–•••

Journal of Differential Equations

www.elsevier.com/locate/jde

Global dynamics of the Josephson equation in TS^1

Hebai Chen [a,*], Yilei Tang [b]

[a] School of Mathematics and Statistics, Central South University, Changsha, Hunan 410083, PR China
[b] School of Mathematical Sciences, MOE-LSC, Shanghai Jiao Tong University, Shanghai, 200240, PR China

Received 16 January 2020; revised 26 March 2020; accepted 26 March 2020

Abstract

The Josephson equation $\dot{\phi} = y,\ \dot{y} = -\sin\phi + \epsilon\big(a - (1 + \gamma\cos\phi)y\big)$ was researched by Sanders and Cushman (1986) [12] for its phase portraits when $\epsilon > 0$ is small by applying the averaging method. The parameter ϵ can actually be large or even any real number in the practical application of this model. When $|\epsilon|$ is not small, we cannot apply the averaging method because the system is not near-Hamiltonian. For general $\epsilon \in \mathbb{R}$, we present complete dynamics and more complex bifurcations of the Josephson equation in TS^1, including saddle-node bifurcation, Hopf bifurcation, Bogdanov-Takens bifurcation, homoclinic loop bifurcation, two-saddle heteroclinic loop bifurcation, upper saddle connection bifurcation and lower saddle connection bifurcation. Moreover, we prove the monotonicity of bifurcation functions with respect to parameters and the nonexistence of a two-saddle heteroclinic loop for all $a \neq 0$.

MSC: 37J35; 34A05; 34A34; 34C14

Keywords: Limit cycle; Josephson equation; Homoclinic loop; Two-saddle loop; Saddle connection

1. Introduction and main results

For planar vector fields with trigonometric functions, there are no general techniques or methods to investigate their dynamics. Although some of these vector fields look simple, the

* Corresponding author.
E-mail addresses: chen_hebai@csu.edu.cn (H. Chen), mathtyl@sjtu.edu.cn (Y. Tang).

https://doi.org/10.1016/j.jde.2020.03.048
0022-0396/

Please cite this article in press as: H. Chen, Y. Tang, Global dynamics of the Josephson equation in TS^1, J. Differential Equations (2020), https://doi.org/10.1016/j.jde.2020.03.048

phenomena of their dynamics can still be very interesting. For example, the one-parameter planar differential equation

$$\ddot{x} + \mu \sin \dot{x} + x = 0, \quad x, \mu \in \mathbb{R}, \tag{1}$$

which has been investigated by many mathematicians, such as [3,10] and [14, Section 4.7], displays rich and complex dynamics. With the transformation $(x, \dot{x}, t) \to (y, x, -t)$, equation (1) is changed into the following system:

$$\dot{x} = y + \mu \sin x, \quad \dot{y} = -x. \tag{2}$$

Eckweiler in [5] conjectured that system (2) has an infinite number of limit cycles. Hochstadt and Stephan in [10] proved that system (2) has an infinite number of limit cycles for sufficiently small $|\mu|$. Later, D'Heedene in [3] obtained the same result for general $\mu \in \mathbb{R}$. According to [14, Section 4.7], system (2) has exactly n limit cycles for $|x| \leq (n+1)\pi$ and $n \in \mathbb{N}$.

As shown in [12], the Josephson equation is of the form

$$\beta \frac{d^2\phi}{dt^2} + (1 + \gamma \cos \phi) \frac{d\phi}{dt} + \sin \phi = \alpha, \tag{3}$$

where $\phi \in S^1$ and $(\alpha, \beta, \gamma) \in \mathbb{R}^3$. Note that system (3) includes two trigonometric functions and three parameters. System (3) can describe a single point contact Josephson junction. See [11,13] and references therein for the applications of point contact Josephson junctions, where the junctions can be used as precision voltage sources. When α is small and $\beta = 1/\epsilon^2$ is large, with the transformation $(\alpha, t) \to (\tilde{\alpha}\epsilon, t\epsilon)$, system (3) can be rewritten as

$$\begin{aligned} \dot{\phi} &= y, \\ \dot{y} &= -\sin \phi + \epsilon\big(\tilde{\alpha} - (1 + \gamma \cos \phi) y\big), \end{aligned} \tag{4}$$

where $\phi \in S^1$. Sanders and Cushman in [12] studied the bifurcation diagram and the phase portraits of system (4) when $\epsilon > 0$ is sufficiently small by the averaging method. Recently, research on the dynamics of similar forms, such as system (4) has attracted great interests from many authors. For example, Gasull, Geyer and Mañosas in [6] studied the number of limit cycles of the more general system

$$\begin{aligned} \dot{x} &= y, \\ \dot{y} &= -\sin x + \epsilon \textstyle\sum_{s=0}^{m} Q_{n,s}(x) y^s \end{aligned}$$

than system (4) by the averaging method, where $Q_{n,s}$ are Fourier polynomials of degree n and $\epsilon > 0$ is small. Furthermore, Gasull, Giné and Valls in [7] studied the center problem of the second order trigonometric differential equation

$$\begin{aligned} \dot{\theta} &= y, \\ \dot{y} &= g(\theta) + y f(\theta), \end{aligned} \tag{5}$$

where $f(0) = g(0) = 0$, $g'(0) < 0$ and f, g are trigonometric polynomial functions. Recently, Gasull, Giné and Valls in [8] obtained an upper bound of the maximum order of the weak focus

Please cite this article in press as: H. Chen, Y. Tang, Global dynamics of the Josephson equation in TS^1, J. Differential Equations (2020), https://doi.org/10.1016/j.jde.2020.03.048

of equations (5) only in terms of the degrees of the involved trigonometric polynomials, when (5) is a pure trigonometric Liénard system.

To apply the averaging method, $\beta \to +\infty$ and $|\alpha|$ must be small to guarantee that system (4) is near-Hamiltonian. However, in practical applications, the parameters $(\alpha, \beta, \gamma) \in \mathbb{R}^3$ are actually general. Naturally, we have the following question:

What is the global dynamics of system (4) *for* $(\alpha, \beta, \gamma) \in \mathbb{R}^3$?

Note that the original differential equation (3) of system (4) is of first order and its dynamics is simple when $\beta = 0$. Therefore, we only consider the case $\beta > 0$ since equation (3) is invariant under the transformation $(\phi, \dot{\phi}, t, \alpha, \beta, \gamma) \to (\phi + \pi, -\dot{\phi}, -t, -\alpha, -\beta, -\gamma)$ when $\beta < 0$. Moreover, we let $\alpha \geq 0$, since equation (3) is invariant under the transformation $(\phi, \dot{\phi}, \alpha) \to (-\phi, -\dot{\phi}, \alpha)$ when $\alpha < 0$. Therefore, we consider the case $\alpha \geq 0$, $\beta > 0$ and $\gamma \in \mathbb{R}$ for equation (3). This is equivalent to considering the general case $\tilde{\alpha} > 0$, $\epsilon > 0$ and $\gamma \in \mathbb{R}$ for system (4). Letting $(a, b, c) := (\tilde{\alpha}\epsilon, \epsilon, \gamma\epsilon)$, we change system (4) into

$$\begin{aligned} \dot{x} &= y, \\ \dot{y} &= -g(x) - f(x)y, \end{aligned} \tag{6}$$

where

$$g(x) = \sin x - a, \qquad f(x) = b + c\cos x,$$

ϕ is replaced by $x \in S^1$, and

$$(a, b, c) \in \mathcal{G} := [0, +\infty) \times (0, +\infty) \times \mathbb{R}.$$

The main results of this paper for system (6) are given as follows.

Theorem 1. *The parameter space* $\mathcal{G}$ *of system* (6) *includes the following local and global bifurcation surfaces and curves, and cross-sections of the bifurcation diagram are as shown in* Fig. 1 *for an arbitrarily fixed constant* c_0*:*

(a): *Saddle-node bifurcation surface*

$$SN := \{(a, b, c) \in \mathcal{G} : a = 1\}.$$

(b): *Hopf bifurcation surface*

$$H := \{(a, b, c) \in \mathcal{G} : b = -c\sqrt{1 - a^2},\ 0 \leq a < 1\}.$$

(c): *Bogdanov-Takens bifurcation curve*

$$BT := \{(a, b, c) \in \mathcal{G} : a = 1,\ b = 0,\ c < 0\}.$$

(d): *The bifurcation surface of the homoclinic loop*

$$HL := \{(a, b, c) \in \mathcal{G} : b = \varphi(a, c),\ 0 < a < 1,\ c < 0\},$$

Please cite this article in press as: H. Chen, Y. Tang, Global dynamics of the Josephson equation in TS^1, J. Differential Equations (2020), https://doi.org/10.1016/j.jde.2020.03.048

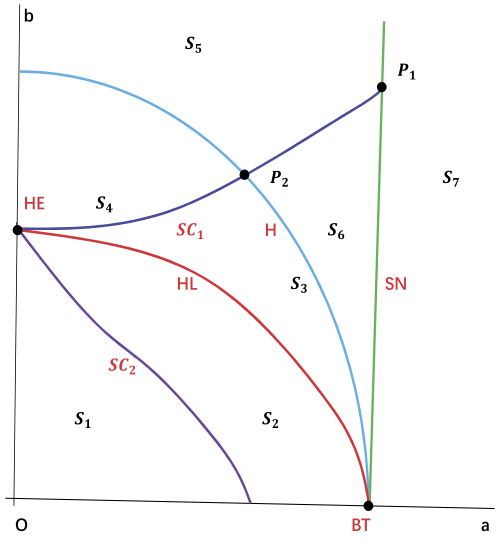

(a) when $c = c_0 < 0$

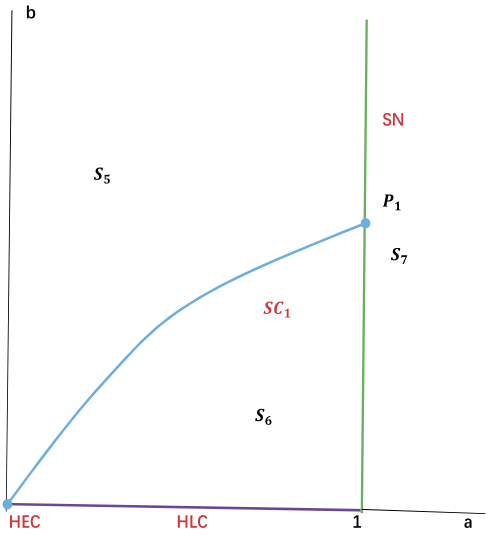

(b) when $c = 0$

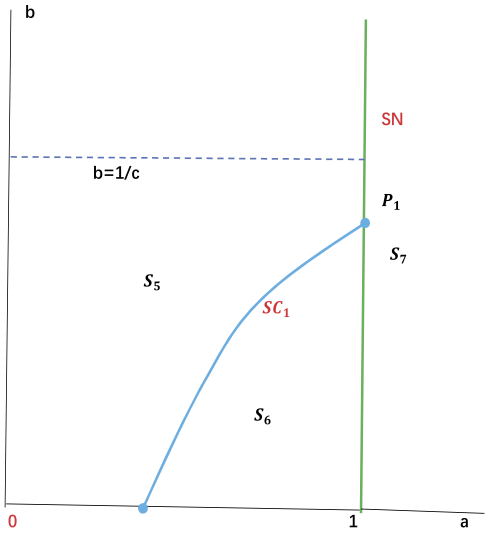

(c) when $c = c_0 > 0$

Fig. 1. Cross-sections of the bifurcation diagram of system (6).

where $\varphi \in C^0$, $\varphi(1,c) = 0$, $0 < \varphi(a,c) < -c\sqrt{1-a^2}$ *for* $0 < a < 1$ *and* $c < 0$, *and*

$$\varphi(a,c) = -5c\sqrt{2(1-a)}/7 + o(-c\sqrt{1-a})$$

when $-c\sqrt{1-a}$ *is sufficiently small.*

(e): *The bifurcation curve of the* 2*-saddle heteroclinic loop*

$$HE := \{(a,b,c) \in \mathcal{G} : b = \varphi(0,c),\ a = 0,\ c < 0\}.$$

Please cite this article in press as: H. Chen, Y. Tang, Global dynamics of the Josephson equation in TS^1, J. Differential Equations (2020), https://doi.org/10.1016/j.jde.2020.03.048

(f): *The bifurcation surface of the upper saddle connection*

$$SC_1 := \{(a,b,c) \in \mathcal{G} : b = \psi_1(a,c),\ 0 < a < 1\},$$

where $\psi_1(0,c) = \varphi(0,c)$, $\psi_1(a,c) > \varphi(a,c)$ *for* $0 < a < 1$ *and* $c < 0$, *and* $\psi_1 \in \mathcal{C}^0$ *is increasing with respect to* a. *In addition, there exists a unique constant* a^* *satisfying* $\psi_1(a^*,c) = -c\sqrt{1-a^{*2}}$.

(g): *The bifurcation surface of the lower saddle connection*

$$SC_2 := \{(a,b,c) \in \mathcal{G} : b = \psi_2(a,c),\ 0 < a < a_* < 1,\ c < 0\}$$

for a unique constant $a_* \in (0,1)$, *where* $\psi_2(0,c) = \varphi(0,c)$, $\psi_2(a_*,c) = 0$, $0 < \psi_2(a,c) < \varphi(a,c)$ *for* $0 < a < a_*$ *and* $c < 0$, *and* $\psi_2 \in C^0$ *is decreasing with respect to* a.

The complete classification of the phase portraits of system (6) *is given in* Fig. 2, *where*

$$\begin{aligned}
S_1 &:= \{(a,b,c) \in \mathcal{G} :\ 0 < b < \psi_2(a,c),\ 0 < a < a_*,\ c < 0\},\\
S_2 &:= \{(a,b,c) \in \mathcal{G} :\ \psi_2(a,c) < b < \varphi(a,c),\ 0 < a < a_*,\ c < 0\}\\
&\quad \cup\{(a,b,c) \in \mathcal{G} :\ 0 < b < \varphi(a,c),\ a_* \le a < 1,\ c < 0\},\\
S_3 &:= \{(a,b,c) \in \mathcal{G} :\ \varphi(a,c) < b < \psi_1(a,c),\ 0 < a < a^*,\ c < 0\}\\
&\quad \cup\{(a,b,c) \in \mathcal{G} :\ \varphi(a,c) < b < -c\sqrt{1-a^2},\ a^* \le a < 1,\ c < 0\},\\
S_4 &:= \{(a,b,c) \in \mathcal{G} :\ \psi_1(a,c) < b < -c\sqrt{1-a^2},\ 0 < a < a^*,\ c < 0\},\\
S_5 &:= \{(a,b,c) \in \mathcal{G} :\ b \ge -c\sqrt{1-a^2},\ 0 < a < a^*,\ c < 0\}\\
&\quad \cup\{(a,b,c) \in \mathcal{G} :\ b > \psi_1(a,c),\ a^* \le a < 1,\ c < 0\}\\
&\quad \cup\{(a,b,c) \in \mathcal{G} :\ b > \max\{\psi_1(a,c),0\},\ 0 < a < 1,\ c \ge 0\},\\
S_6 &:= \{(a,b,c) \in \mathcal{G} :\ -c\sqrt{1-a^2} \le b < \psi_1(a,c),\ a^* < a < 1,\ c < 0\}\\
&\quad \cup\{(a,b,c) \in \mathcal{G} :\ 0 < b < \psi_1(a,c),\ 0 < a < 1,\ c \ge 0\},\\
S_7 &:= \{(a,b,c) \in \mathcal{G} :\ a > 1\},\\
SC_{11} &:= \{(a,b,c) \in \mathcal{G} : b = \psi_1(a,c),\ a^* \le a < 1, c < 0\}\\
&\quad \cup\{(a,b,c) \in \mathcal{G} :\ b = \psi_1(a,c),\ 0 < a < 1,\ c \ge 0\},\\
SC_{12} &:= \{(a,b,c) \in \mathcal{G} : b = \psi_1(a,c),\ 0 < a < a^*, c < 0\},\\
P_1 &:= \{(a,b,c) \in \mathcal{G} : a = 1, b = \psi_1(1,c), c < 0\},\\
SN_1 &:= \{(a,b,c) \in \mathcal{G} : a = 1, b > \psi_1(1,c)\}\\
SN_2 &:= \{(a,b,c) \in \mathcal{G} : a = 1, 0 < b < \psi_1(1,c)\},\\
HEC &:= \{(a,b,c) \in \mathcal{G} :\ a = b = c = 0\},\\
HLC &:= \{(a,b,c) \in \mathcal{G} :\ 0 < a < 1,\ b = c = 0\}.
\end{aligned}$$

Please cite this article in press as: H. Chen, Y. Tang, Global dynamics of the Josephson equation in TS^1, J. Differential Equations (2020), https://doi.org/10.1016/j.jde.2020.03.048

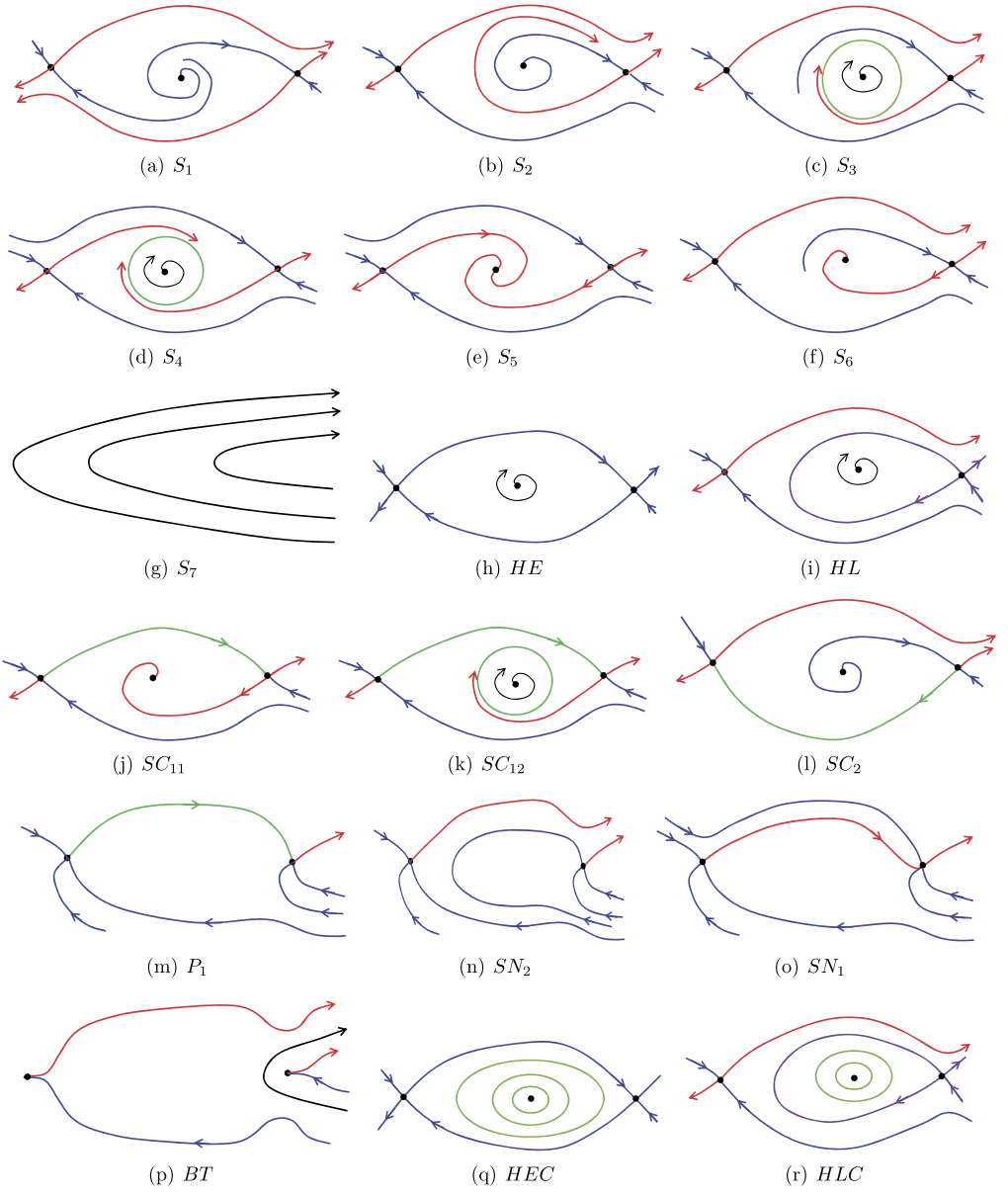

Fig. 2. Phase portraits of system (6).

Remark 1. Note that the phase portraits in Fig. 2 (g, m-p, r) for local and non-local parameters have not been presented in [12]. In Figure 3 of [12, P. 499], when system (4) has an upper saddle connection, the direction of vector fields in the phase portraits is clockwise not counterclockwise, as presented in Fig. 2 (j, k).

The paper is organized as follows. In Section 2, we give local bifurcations and dynamics of system (6). In Section 3, we research the problems of limit cycles and saddle connections of

Please cite this article in press as: H. Chen, Y. Tang, Global dynamics of the Josephson equation in TS^1, J. Differential Equations (2020), https://doi.org/10.1016/j.jde.2020.03.048

system (6), and further present its global bifurcations and dynamics. The last section is devoted to the proof of our main results, i.e., Theorem 1. Moreover, our theoretical results are illustrated by some numerical simulations.

2. Local bifurcations

In this section, we describe all local bifurcations of system (6).

Theorem 2. *We find the local bifurcation surfaces and curves in parameter space $\mathcal{G}$ of system (6) as follows*

(a): *There is a saddle-node bifurcation surface SN when $a = 1$. When $a > 1$, system (6) has no equilibria. When $0 \le a < 1$, system (6) has three equilibria*

$$E_l = (-\pi - \arcsin a, 0), \quad E_0 = (\arcsin a, 0), \quad E_r = (\pi - \arcsin a, 0)$$

for $x \in [-\pi - \arcsin a, \pi - \arcsin a]$, where E_0 is an anti-saddle and $E_{l,r}$ are saddles. When $a = 1$, system (6) has two equilibria $E_l = (-3\pi/2, 0)$ and $E_r = (\pi/2, 0)$ for $x \in [-3\pi/2, \pi/2]$, which are saddle-nodes.

(b): *There is a Hopf bifurcation surface H for the equilibrium at E_0 when*

$$b = -c\sqrt{1-a^2} \text{ and } 0 \le a < 1.$$

A limit cycle can bifurcate from this equilibrium for $0 \le a < 1$ and sufficiently small $-(b + c\sqrt{1-a^2}) > 0$.

(c): *The intersection of H and HL defines Bogdanov-Takens bifurcation curve BT as $a = 1$, $b = 0$ and $c < 0$, where the local bifurcation surface of homoclinic loop HL is represented by $b = -5c\sqrt{2(1-a)}/7 + o(\sqrt{1-a})$.*

Proof. **(a)** Note that the equilibria of system (6) are solved by the equations

$$\{y = 0, \quad -\sin x + a = 0\}.$$

For $x \in [-\pi - \arcsin a, \pi - \arcsin a]$, system (6) has two equilibria at $E_l = (-3\pi/2, 0)$ and $E_r = (\pi/2, 0)$ when $a = 1$; three equilibria at $E_l = (-\pi - \arcsin a, 0)$, $E_0 = (\arcsin a, 0)$ and $E_r = (\pi - \arcsin a, 0)$ when $0 \le a < 1$; and no equilibria when $a > 1$. Note that the Jacobian matrix at a general equilibrium E of system (6) is

$$J_E = \begin{pmatrix} 0 & 1 \\ -\cos x & -(b + c\cos x) \end{pmatrix}.$$

Then, for $0 \le a < 1$ equilibria $E_{l,r}$ are saddles and equilibrium E_0 is a focus, node or center according to a classical and easy analysis of the eigenvalues of J_{E_l}, J_{E_r} and J_{E_0}.

When $a = 1$, the determinants of J_{E_l} and J_{E_r} satisfy that $\mathcal{D}et(J_{E_l}) = 0 = \mathcal{D}et(J_{E_r})$. Moreover, applying the Taylor expansion, we have

Please cite this article in press as: H. Chen, Y. Tang, Global dynamics of the Josephson equation in TS^1, J. Differential Equations (2020), https://doi.org/10.1016/j.jde.2020.03.048

$$a-\sin x = a-1+\frac{1}{2}(x-\frac{\pi}{2})^2-\frac{1}{4!}(x-\frac{\pi}{2})^4+O(|x-\frac{\pi}{2}|^6), \tag{7}$$
$$\left(resp.\ a-\sin x = a-1+\frac{1}{2}(x+\frac{3\pi}{2})^2-\frac{1}{4!}(x+\frac{3\pi}{2})^4+O(|x+\frac{3\pi}{2}|^6)\right)$$

in the small neighborhood of $x=\pi/2$ (resp. $x=-3\pi/2$). From (7), the canonical form of system (6) becomes

$$\dot{x} = -\frac{1}{2b^2}x^2+(\frac{1}{b^2}-\frac{c}{b})xy+(-\frac{1}{2b^2}+\frac{c}{b})y^2+O(|(x,y)|^4),$$
$$\dot{y} = -by-\frac{1}{2b^2}x^2+(\frac{1}{b^2}-\frac{c}{b})xy+(-\frac{1}{2b^2}+\frac{c}{b})y^2+O(|(x,y)|^4)$$

after the change $(x-(1/2)\pi, y)\to((y-x)/b, -y)$. Then, equilibrium E_r is a saddle-node when $a=1$. By a similar analysis, we obtain that equilibrium E_l is also a saddle-node when $a=1$.

(b) When $0\le a<1$, a Hopf bifurcation can occur at equilibrium $E_0=(\arcsin a, 0)$ because the trace of matrix J_{E_0} is $-b-c\sqrt{1-a^2}$ and vanishes when $b=-c\sqrt{1-a^2}$. Thus, we have $c<0$ by $b>0$. Localizing system (6) at E_0 and making the transformation $(x,y)\to(x+\arcsin a, y)$, we change system (6) into

$$\begin{aligned}&\dot{x} = y,\\ &\dot{y} = -\sqrt{1-a^2}x+\tfrac{a}{2}x^2+acxy+\tfrac{\sqrt{1-a^2}}{6}x^3+\tfrac{c\sqrt{1-a^2}}{2}x^2y+O(|(x,y)|^4).\end{aligned} \tag{8}$$

Further, with the transformation

$$(y,t)\to\left(\sqrt[4]{1-a^2}y, \frac{t}{\sqrt[4]{1-a^2}}\right),$$

system (8) is changed into

$$\begin{aligned}&\dot{x} = y,\\ &\dot{y} = -x+\tfrac{a}{2\sqrt{1-a^2}}x^2+\tfrac{ac}{\sqrt[4]{1-a^2}}xy+\tfrac{1}{6}x^3+\tfrac{c\sqrt[4]{1-a^2}}{2}x^2y+O(|(x,y)|^4).\end{aligned} \tag{9}$$

By using the formula given in [2, p. 211], we compute the first Lyapunov value g_3 for system (9) and obtain

$$g_3=\frac{c\sqrt[4]{(1-a^2)^{-3}}}{16}<0,$$

which implies that $(0,0)$ of system (9) is a stable weak focus of multiplicity one. Note that the equilibrium E_0 of system (6) is an unstable focus for sufficiently small $-(b+c\sqrt{1-a^2})>0$. Therefore, we obtain the Hopf bifurcation surface H and a stable limit cycle can bifurcate from E_0 for $0\le a<1$ and sufficiently small $-(b+c\sqrt{1-a^2})>0$.

(c) The Bogdanov-Takens bifurcation occurs when the divergence vanishes at a double zero point. When $a=1$, $b=0$ and $c<0$, system (8) becomes

Please cite this article in press as: H. Chen, Y. Tang, Global dynamics of the Josephson equation in TS^1, J. Differential Equations (2020), https://doi.org/10.1016/j.jde.2020.03.048

$$\dot{x} = y,$$
$$\dot{y} = \tfrac{1}{2}x^2 + cxy + O(|(x, y)|^4),$$

which indicates that equilibrium $E_r (= E_0)$ of system (6) is a cusp. By a similar discussion, equilibrium E_l of system (6) is also a cusp. With the transformation $(x, y) \to (x + \pi/2, y)$ for general parameters (a, b, c), we locate system (6) at $(x, y) = (0, 0)$ and have

$$\begin{aligned} &\dot{x} = y, \\ &\dot{y} = a - 1 - by + \tfrac{1}{2}x^2 + cxy + O(|(x, y)|^4). \end{aligned} \tag{10}$$

With the scaling

$$(x, y, t) \to \left(\frac{1}{2c^2}x, \frac{1}{4c^3}y, 2ct\right),$$

system (10) can be rewritten as

$$\dot{x} = y,$$
$$\dot{y} = \mu_1 + \mu_2 y + x^2 + xy + O(|x, y|^4),$$

where

$$(\mu_1, \mu_2) := \left(8c^4(a - 1), -2bc\right).$$

By Theorem 1.2 of [2, Chapter 4], the homoclinic bifurcation curve is

$$\mu_1 = -\frac{49}{25}\mu_2^2 + O(|\mu_2|^{5/2}), \quad \mu_2 > 0$$

for small enough $|\mu_1|$ and $|\mu_2|$, i.e., $b = -5c\sqrt{2(1 - a)}/7 + o(-c\sqrt{1 - a})$. □

3. Limit cycles, saddle connections and global bifurcation

In this section, we study the limit cycles and saddle connections of system (6). For simplicity, the parameter space $\mathcal{G}$ is divided into the following regions:

$$\begin{aligned} \mathcal{G}_1 &:= \{(a, b, c) \in \mathcal{G} : a \geq 1\}, \\ \mathcal{G}_2 &:= \{(a, b, c) \in \mathcal{G} : 0 \leq a < 1,\ b \geq -c\}, \\ \mathcal{G}_3 &:= \{(a, b, c) \in \mathcal{G} : 0 \leq a < 1,\ b < -c\sqrt{1 - a^2},\ c < 0\}, \\ \mathcal{G}_4 &:= \{(a, b, c) \in \mathcal{G} : 0 \leq a < 1,\ -c\sqrt{1 - a^2} \leq b < -c,\ c < 0\}. \end{aligned}$$

We find that no limit cycles exist in the parameter regions $\mathcal{G}_1$, $\mathcal{G}_2$ and $\mathcal{G}_4$.

Lemma 3. *System* (6) *has no limit cycles when* $(a, b, c) \in \mathcal{G}_1$.

Please cite this article in press as: H. Chen, Y. Tang, Global dynamics of the Josephson equation in TS^1, J. Differential Equations (2020), https://doi.org/10.1016/j.jde.2020.03.048

Proof. By Theorem 2, system (6) has no equilibria when $a > 1$, implying that no limit cycles exist in this case. Moreover, system (6) has two equilibria E_l and E_r for $x \in [-3\pi/2, \pi/2]$ when $a = 1$, which are saddle-nodes. By [14, Chapter 3], the index of any saddle-node is 0 and the sum of the index of all equilibria surrounded by any limit cycle is $+1$. Therefore, system (6) has no limit cycles when $a = 1$. □

Lemma 4. *System (6) has no limit cycles when* $(a, b, c) \in \mathcal{G}_2$.

Proof. When $(a, b, c) \in \mathcal{G}_2$, we have $0 \le a < 1$ and $b \ge -c$. First, we consider the case $-b \le c \le b$. Note that the divergence of the vector field of (6) is $-b - c\cos x \le 0$. Thus, from the Dulac criterion in [14, Chapter 4], system (6) has no limit cycles when $-b \le c \le b$.

Next, we consider the case $c > b$. With the global transformation $(x, y) \to (x, y - F(x))$, system (6) is changed into

$$\dot{x} = y - F(x), \qquad \dot{y} = -g(x), \tag{11}$$

for $x \in S^1$, where

$$F(x) = bx + c\sin x, \qquad f(x) = F'(x) = b + c\cos x$$

and $g(x)$ is shown in (6). When $c > b$, with the transformation

$$(x, y) \to (x + \arcsin a, y + b\arcsin a + ac),$$

we move the equilibrium $E_C = (\arcsin a, b\arcsin a + ac)$ of system (11) to the origin and system (11) is rewritten as

$$\dot{x} = y - F_a(x), \qquad \dot{y} = -g_a(x), \tag{12}$$

where

$$F_a(x) = bx + c\sin(x + \arcsin a) - ac, \quad g_a(x) = \sin(x + \arcsin a) - a$$

and $-\pi - 2\arcsin a < x < \pi - 2\arcsin a$. Let

$$\Phi(x, y) := G(x) + \frac{y^2}{2} = -\cos(x + \arcsin a) + \sqrt{1 - a^2} - ax + \frac{y^2}{2}, \tag{13}$$

where $G(x) := \int_0^x g_a(s)ds$. It follows from (13) that

$$\begin{aligned} \frac{d\Phi}{dt}|_{(12)} &= -g_a(x)F_a(x) \\ &= -\big(\sin(x + \arcsin a) - a\big)\big(bx + c\sin(x + \arcsin a) - ac\big) \\ &= -c\big(\sin(x + \arcsin a) - a\big)^2 - bx\big(\sin(x + \arcsin a) - a\big) \\ &\le 0 \end{aligned} \tag{14}$$

Please cite this article in press as: H. Chen, Y. Tang, Global dynamics of the Josephson equation in TS^1, J. Differential Equations (2020), https://doi.org/10.1016/j.jde.2020.03.048

in the strip $-\pi - 2\arcsin a < x < \pi - 2\arcsin a$. Assume that system (12) exhibits a limit cycle γ in strip $-\pi - 2\arcsin a < x < \pi - 2\arcsin a$. Clearly, we have

$$\oint_{\gamma} d\Phi = 0.$$

However, we can obtain from (14) that

$$\oint_{\gamma} d\Phi = \oint_{\gamma} -g_a(x)F_a(x)dt < 0,$$

indicating a contradiction. Therefore, system (6) has no limit cycles when $(a, b, c) \in \mathcal{G}_2$ □

Lemma 5. *System (6) has at most one limit cycle in interval $-\pi - \arcsin a < x < \pi - \arcsin a$ when $(a, b, c) \in \mathcal{G}_3$. Moreover, the limit cycle is stable and hyperbolic if it exists.*

Proof. It follows from $c < -b/\sqrt{1-a^2}$ that

$$\sqrt{a^2 + \frac{b^2}{c^2}} < \sqrt{a^2 + 1 - a^2} = 1.$$

Therefore, by system (6), we have

$$\begin{aligned} \frac{d(f(x)/g(x))}{dx} &= c\frac{d(\frac{b/c+\cos x}{\sin x - a})}{dx} \\ &= c\frac{-\sin x(\sin x - a) - (b/c + \cos x)\cos x}{(\sin x - a)^2} \\ &= c\frac{a\sin x - b\cos x/c - 1}{(\sin x - a)^2} \\ &= c\frac{\sqrt{a^2 + \frac{b^2}{c^2}}\sin(x + x_0) - 1}{(\sin x - a)^2} > 0 \end{aligned} \tag{15}$$

for $x \in (-\pi - \arcsin a, \arcsin a) \cup (\arcsin a, \pi - \arcsin a)$, $0 \le a < 1$ and $c < 0$, where $\sin x_0 = b/\sqrt{a^2c^2 + b^2}$. Note that $(x - \arcsin a)g(x) > 0$ for $x \neq \arcsin a$.

Now, consider the equivalent systems (11) and (12) of system (6). Let

$$z(x) := \int_0^x g_a(s)ds = -\cos(x + \arcsin a) + \sqrt{1-a^2} - ax.$$

Then, we have the two inverse branch functions $x = x_1(z)$ for $0 < x < \pi - 2\arcsin a$ and $x = x_2(z)$ for $-\pi - 2\arcsin a < x < 0$. Furthermore, in strip $-\pi - 2\arcsin a < x < \pi - 2\arcsin a$, system (12) can be changed into

Please cite this article in press as: H. Chen, Y. Tang, Global dynamics of the Josephson equation in TS^1, J. Differential Equations (2020), https://doi.org/10.1016/j.jde.2020.03.048

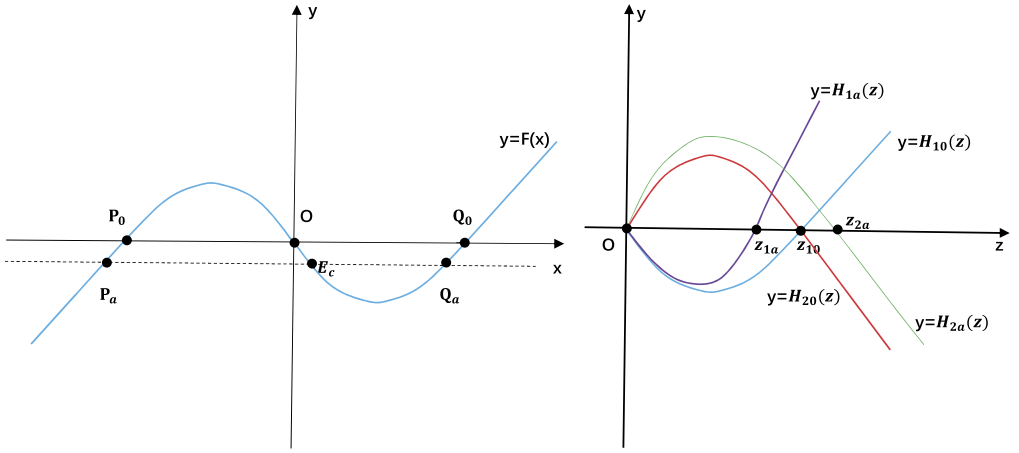

(a) xy-plane (b) zy-plane

Fig. 3. $y = F(x)$ and equilibrium E_C of system (11).

$$\frac{dz}{dy} = F_a(x_1(z)) - y =: H_{1a}(z) - y,$$
$$\frac{dz}{dy} = F_a(x_2(z)) - y =: H_{2a}(z) - y$$

by the transformation $(x, y) \to (z, y)$.

First, we need to present the relative position of the images of $H_{1a}(z)$ and $H_{2a}(z)$ in the zy-plane to obtain the existence and uniqueness of limit cycles. Fig. 3(a) depicts the image curve for the function $y = F(x)$, which becomes the curve $y = F_a(x)$ after moving the equilibrium E_C of system (11) to the origin of system (12). Note that the function $y = F(x)$ has three zeros at P_0, Q_0 and the origin O on the x-axis, and has the same negative function value at three other points P_a, Q_a and equilibrium E_C. Moreover, the abscissa of E_C increases and the abscissae of P_a and Q_a decrease when a increases. In the zy-plane, the curves $y = H_{1a}(z)$ and $y = H_{2a}(z)$ are shown in Fig. 3(b), which are translated from the curve $y = F_a(x)$ by the transformation $(x, y) \to (z, y)$. Note that the curves $y = H_{1a}(z)$ and $y = H_{2a}(z)$ become the curves $y = H_{10}(z)$ and $y = H_{20}(z)$ when $a = 0$, respectively.

Since $F_a(x)$ has exactly one positive zero and one negative zero, the curve $H_{1a}(z)$ (resp. $H_{2a}(z)$) has a unique positive zero at z_{1a} (resp. z_{2a}). Moreover, $(z - z_{1a})H_{1a}(z) > 0$ for $z \in (0, z_{1a}) \cup (z_{1a}, +\infty)$ and $(z - z_{2a})H_{2a}(z) > 0$ for $z \in (0, z_{2a}) \cup (z_{2a}, +\infty)$. Note that $z_{1a} = z_{2a} = z_{10}$ for $a = 0$.

In the following, we prove that $z_{1a} < z_{2a}$ for $0 < a < 1$. Assume that there is an $a \in (0, 1)$ such that $z_{1a} = z_{2a}$. Then, we have

$$F_a(x_{1a}) = F_a(x_{2a}) \text{ and } G_a(x_{1a}) = G_a(x_{2a}), \tag{16}$$

where $F_a(x_{1a}) = F_a(x_{2a}) = 0$. By (16), it follows that

$$bx_{1a} + c\sin(x_{1a} + \arcsin a) = bx_{2a} + c\sin(x_{2a} + \arcsin a) \tag{17}$$

and

Please cite this article in press as: H. Chen, Y. Tang, Global dynamics of the Josephson equation in TS^1, J. Differential Equations (2020), https://doi.org/10.1016/j.jde.2020.03.048

$$ax_{1a} + \cos(x_{1a} + \arcsin a) = ax_{2a} + \cos(x_{2a} + \arcsin a). \tag{18}$$

It follows from (17) and (18) that

$$\begin{aligned} &\sin(x_{1a} + \arcsin a + \arcsin \frac{b}{\sqrt{a^2c^2 + b^2}}) \\ &= \sin(x_{2a} + \arcsin a + \arcsin \frac{b}{\sqrt{a^2c^2 + b^2}}). \end{aligned} \tag{19}$$

Since $0 < b < -c\sqrt{1 - a^2}$, we can obtain

$$0 < \arcsin a + \arcsin \frac{b}{\sqrt{a^2c^2 + b^2}} < \frac{\pi}{2}.$$

Further, by (19) we have

$$\chi := x_{1a} + x_{2a} + 2\arcsin a + 2\arcsin \frac{b}{\sqrt{a^2c^2 + b^2}} = 2k\pi + \pi, \quad k \in \mathbb{Z}.$$

Moreover, applying $-\pi - 2\arcsin a < x_{2a} < 0 < x_{1a} < \pi - 2\arcsin a$, we obtain $\chi \in (-\pi, 2\pi)$ and then $k = 0$. Thus, we obtain

$$\chi = \pi \tag{20}$$

There exists a unique $x_0 \in (0, \pi - \arcsin a)$ such that $F(\pm x_0) = 0$. Since $x_{1a} < x_0$ and $x_{2a} < -x_0$, we have $x_{1a} + x_{2a} < 0$ and

$$\chi = x_{1a} + x_{2a} + 2\arcsin a + 2\arcsin \frac{b}{\sqrt{a^2c^2 + b^2}} < \pi,$$

which contradicts equality (20). Therefore, we have proven that $z_{1a} < z_{2a}$ for $0 < a < 1$.

By Proposition 2.1 of [1], system (12) has no closed orbits in the region $x \in [x_2(z_{1a}), x_{1a}]$ and a closed orbit of system (12) must surround the two points $(x_{1a}, 0)$ and $(x_2(z_{1a}), F_a(x_2(z_{1a})))$ if the closed orbit exists.

Next, we claim that system (12) has at most one limit cycle in interval $(-\arccos(-b/c), \pi - 2\arcsin a)$. Moreover, the limit cycle is stable and hyperbolic if it exists. Note that $F_a'(x)$ has a unique zero at $x = \arccos(-b/c) - \arcsin a$ and that $F_a(x)$ has a unique positive zero in the interval $(-\arccos(-b/c) - \arcsin a, \pi - 2\arcsin a)$. By the monotonicity of $f(x)/g(x)$ with respect to x in (15), the simultaneous equations

$$F_a(x_1) = F_a(x_2), \qquad \frac{F_a'(x_1)}{g_a(x_1)} = \frac{F_a'(x_2)}{g_a(x_2)}$$

have at most one dual solution $\{x_1, x_2\}$ satisfying $-\arccos(-b/c) < x_1 < 0 < x_2 < \pi - 2\arcsin a$. Moreover, $F_a(x)F_a'(x)/g_a(x)$ decreases for $x \in (-\arccos(-b/c) - \arcsin a, 0)$. Thus, by Theorem 2.1 of [4], the claim is proven.

Please cite this article in press as: H. Chen, Y. Tang, Global dynamics of the Josephson equation in TS^1, J. Differential Equations (2020), https://doi.org/10.1016/j.jde.2020.03.048

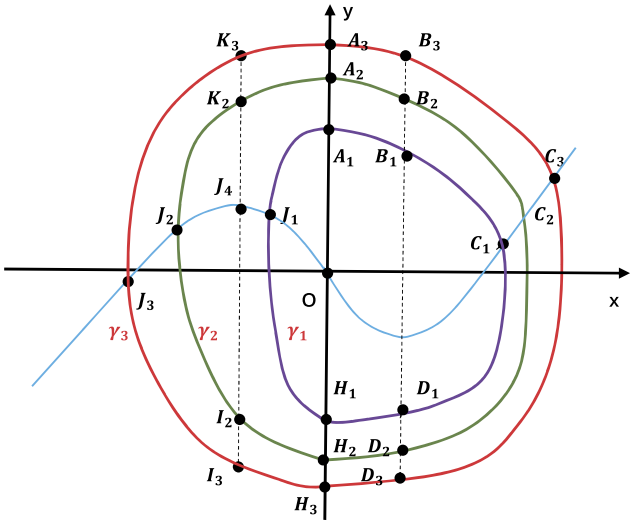

Fig. 4. Limit cycles of system (12) for parameter region $\mathcal{G}_3$.

In the following, we verify the uniqueness of limit cycles of system (12) when $(a, b, c) \in \mathcal{G}_3$. Assume that system (12) has two adjacent limit cycles γ_{int} and γ_{out}, where γ_{int} lies in the interior region surrounded by γ_{out}. We claim that

$$\oint_{\gamma_{out}} F_a'(x)dt > \oint_{\gamma_{int}} F_a'(x)dt. \tag{21}$$

In the first case, we consider that the limit cycles $\gamma_{int} = \gamma_2$ and $\gamma_{out} = \gamma_3$ surround the point $J_4 : (-\arccos(-b/c) - \arcsin a, F_a(-\arccos(-b/c) - \arcsin a))$, where $F_a(x)$ has a maximum value at $-\arccos(-b/c) - \arcsin a < 0$, as shown in Fig. 4. Note that $\gamma_i = A_i B_i C_i \widehat{D_i H_i I_i} J_i K_i A_i$ for $i = 1, 2, 3$, where

$$\begin{aligned} &x_{B_i} = x_{D_i} = \arccos(-b/c) - \arcsin a, \quad x_{K_i} = x_{I_i} = -\arccos(-b/c) - \arcsin a, \\ &y_{C_i} = F_a(x_{C_i}), \qquad y_{J_i} = F_a(x_{J_i}) \qquad x_{A_i} = x_{H_i} = 0. \end{aligned} \tag{22}$$

Letting $y = y_2(x)$ and $y = y_3(x)$ represent the orbit segments $\widehat{K_2A_2B_2}$ and $\widehat{K_3A_3B_3}$ respectively, we have

$$\begin{aligned} \int_{\widehat{K_2A_2B_2}} F_a'(x)dt - \int_{\widehat{K_3A_3B_3}} F_a'(x)dt &= \int_{x_{K_2}}^{x_{B_2}} \left(\frac{F_a'(x)}{y_2 - F_a(x)} - \frac{F_a'(x)}{y_3 - F_a(x)} \right) dx \\ &= \int_{x_{K_2}}^{x_{B_2}} \frac{F_a'(x)(y_3 - y_2)}{(y_2 - F_a(x))(y_3 - F_a(x))} dx \\ &< 0. \end{aligned} \tag{23}$$

Please cite this article in press as: H. Chen, Y. Tang, Global dynamics of the Josephson equation in TS^1, J. Differential Equations (2020), https://doi.org/10.1016/j.jde.2020.03.048

Similarly, we can obtain

$$\int_{\widehat{D_2H_2I_2}} F_a'(x)dt - \int_{\widehat{D_3H_3I_3}} F_a'(x)dt < 0. \tag{24}$$

Using (15), we can obtain that $\big(F_a(x) - F_a(\arccos(-b/c) - \arcsin a\big)F_a'(x)/g_a(x)$ is increasing for $x \in (\arccos(-b/c) - \arcsin a, \pi - 2\arcsin a)$ and $\big(F_a(x) - F_a(-\arccos(-b/c) - \arcsin a)\big)F_a'(x)/g_a(x)$ is increasing for $x \in (-\pi - 2\arcsin a, -\arccos(-b/c) - \arcsin a)$. Then, applying Theorem 2.1 of [4] or Lemma 4.5 of [14, Chapter 4], we have

$$\int_{\widehat{B_2C_2D_2}} F_a'(x)dt - \int_{\widehat{B_3C_3D_3}} F_a'(x)dt < 0 \tag{25}$$

and

$$\int_{\widehat{I_2J_2K_2}} F_a'(x)dt - \int_{\widehat{I_3J_3K_3}} F_a'(x)dt < 0. \tag{26}$$

It follows from (23)-(26) that inequality (21) holds.

In the second case, we consider that system (12) has one limit cycle γ_1 in strip $(-\arccos(-b/c), \pi - 2\arcsin a)$, as shown in Fig. 4. Note that system (12) has at most one limit cycle in this strip according to the aforementioned analysis. Take a closed curve

$$\mathcal{C}_1 := \widehat{H_1J_1A_1} \cup \overline{A_1A_2} \cup \widehat{A_2J_2H_2} \cup \overline{H_2H_1}.$$

It follows from the Green formula that

$$\begin{aligned}\int_{\widehat{H_1J_1A_1}} F_a'(x)dt - \int_{\widehat{H_2J_2A_2}} F_a'(x)dt &= \oint_{\mathcal{C}} F_a'(x)dt \\ &= \oint_{\mathcal{C}} -\frac{F_a'(x)}{g(x)}dy \\ &= \iint_{S(\mathcal{C})} -\frac{\partial(F_a'(x)/g(x))}{\partial x}dxdy < 0,\end{aligned} \tag{27}$$

where $S(\mathcal{C}_1)$ is the region surrounded by $\mathcal{C}_1$. Similarly, we also have

$$\int_{\widehat{A_1C_1H_1}} F_a'(x)dt - \int_{\widehat{A_2C_2H_2}} F_a'(x)dt < 0. \tag{28}$$

By (27)-(28), inequality (21) still holds for the closed orbits γ_1 and γ_2.

Let γ_{int} be the innermost limit cycle surrounding the origin of system (12), and it is internally stable because the origin is a source. It follows from Theorem 2.2 and its Corollary 1 of [14,

Chapter 4] that $\oint_{\gamma_{int}} F_a'(x)dt \geq 0$. Thus, we have $\oint_{\gamma_{out}} F_a'(x)dt > 0$ by (21), implying that γ_{out} is stable. Note that two adjacent limit cycles cannot be simultaneously stable. Therefore, system (12) has at most two limit cycles. Moreover, the inner limit cycle is semistable and the outer one is stable if system (12) has exactly two limit cycles. It is obvious that the vector field of system (12) is generalized rotated with respect to b according to [14, Chapter 4.3]. Assume that system (12) exhibits a semistable limit cycle γ_{int} for $(a, b, c) = (a_0, b_0, c_0)$. By the rotation in b_0, system (12) bifurcates a stable limit cycle $\hat{\gamma}_0$ and an unstable limit cycle $\tilde{\gamma}_0$ in a small neighborhood of γ_{int}, where $\hat{\gamma}_0$ lies in the interior region surrounded by $\tilde{\gamma}_0$. Consequently, we obtain

$$\oint_{\tilde{\gamma}_0} F_a'(x)dt \leq 0 \leq \oint_{\hat{\gamma}_0} F_a'(x)dt.$$

However, we can obtain that $\oint_{\tilde{\gamma}_0} F_a'(x)dt > \oint_{\hat{\gamma}_0} F_a'(x)dt$ from (21). This is a contradiction, indicating that systems (11) and (6) have at most one limit cycle in interval $-\pi - \arcsin a < x < \pi - \arcsin a$ when $(a, b, c) \in \mathcal{G}_3$, which is stable and hyperbolic. The conclusion in this lemma is proven. □

Based on the results in Lemmas 4 and 5, we consider the parameter region $\mathcal{G}_4$ in the following lemma.

Lemma 6. *System (6) has no limit cycles when* $(a, b, c) \in \mathcal{G}_4$.

Proof. First, we prove that the equivalent system (12) of system (6) has no limit cycles for $b = -c\sqrt{1-a^2}$. Assume that there is a dual $\{x_1, x_2\}$ solution satisfying

$$F_a(x_1) = F_a(x_2) \text{ and } G_a(x_1) = G_a(x_2), \tag{29}$$

where $-\pi - 2\arcsin a < x_1 < 0 < x_2 < \pi - 2\arcsin a$. By (29) and $c = -b/\sqrt{1-a^2}$, we have

$$-\sqrt{1-a^2}x_1 + \sin(x_1 + \arcsin a) = -\sqrt{1-a^2}x_2 + \sin(x_2 + \arcsin a) \tag{30}$$

and

$$ax_1 + \cos(x_1 + \arcsin a) = ax_2 + \cos(x_2 + \arcsin a). \tag{31}$$

It follows from (30) and (31) that

$$\sin(x_1 + \arcsin a + \arccos a) = \sin(x_2 + \arcsin a + \arccos a).$$

Further, by $\arcsin a + \arccos a = \pi/2$ and $-\pi - 2\arcsin a < x_1 < 0 < x_2 < \pi - 2\arcsin a$, we have $x_1 = -x_2$. By $x_1 = -x_2$ and (31), we further obtain that $x_1 = \sin x_1$, implying $x_1 = x_2 = 0$. Thus, equations (29) have only the zero dual solution $\{x_1, x_2\}$. By Proposition 2.1 in [1], system (12) has no limit cycles for $c = -b/\sqrt{1-a^2}$.

Second, we prove that system (6) has no limit cycles for $0 < -c\sqrt{1-a^2} < b < -c$. Assume that system (6) has limit cycles for $b = b_0 \in (-c\sqrt{1-a^2}, -c)$ and that Γ is the innermost limit cycle. It follows from the stability of E_C that Γ is internally unstable. Note that

Please cite this article in press as: H. Chen, Y. Tang, Global dynamics of the Josephson equation in TS^1, J. Differential Equations (2020), https://doi.org/10.1016/j.jde.2020.03.048

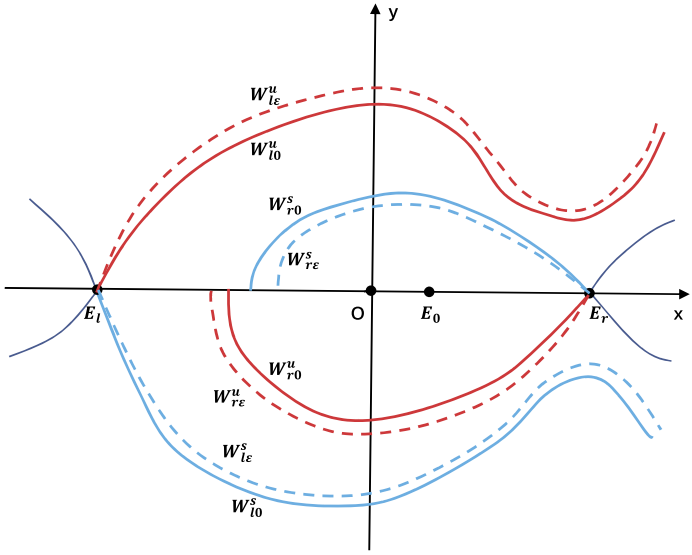

Fig. 5. Manifolds of saddles of system (6) under small perturbations of $b+\epsilon$ when $0 \le a < 1$.

$$\begin{vmatrix} y & -\sin x + a - (b_0 + c\cos x)y \\ y & -\sin x + a - (b + c\cos x)y \end{vmatrix} = (b_0 - b)y^2 \ge 0, \tag{32}$$

where $b \in (b_0, b_0+\epsilon)$ and $\epsilon > 0$ is small. Moreover, the equality for (32) holds if and only if $y = 0$. Thus, analytic system (6) defines a family of generalized rotated vector fields for $(x, y, b) \in \mathbb{R}^3$ by Definition 3.3 in [14]. Therefore, unstable limit cycles of system (6) contract and stable limit cycles expand as b decreases; a semistable limit cycle of system (6) that is internally unstable bifurcates into an unstable one and a stable one as b_0 decreases by Theorem 3.4 of [14, Chapter IV], where the unstable one lies in the interior region surrounded by the stable one. Therefore, in system (6), a new unstable limit cycle occurs in a small interior neighborhood of Γ when $b = b_0 - \delta$, where $\delta > 0$ is small. Further, unless $b = -c\sqrt{1-a^2}$, system (6) still has an unstable limit cycle since E_C remains stable. This is a contradiction and the assertion is proven. □

In strip $-\pi - \arcsin a < x < \pi - \arcsin a$, let W^u_{l0} (or W^s_{l0}) and W^u_{r0} (or W^s_{r0}) be the unstable (or stable) manifold of equilibria $E_l = (-\pi - \arcsin a, 0)$ and $E_r = (\pi - \arcsin a, 0)$ for system (6), respectively. System $(6)|_{b\to b+\epsilon}$ or system $(6)|_{a\to a+\epsilon}$ is regarded as a perturbation of system (6). Let $W^u_{l\epsilon}$ (or $W^s_{l\epsilon}$) and $W^u_{r\epsilon}$ (or $W^s_{r\epsilon}$) be the unstable (or stable) manifold of equilibria E_l and E_r of system $(6)|_{b\to b+\epsilon}$ or system $(6)|_{a\to a+\epsilon}$, respectively.

In the following lemma, we reveal that the stable or unstable manifolds of two saddles of system (6) have some monotonicity with respect to a and b.

Lemma 7. *When $(a, b, c) \in \mathcal{G}_2 \cup \mathcal{G}_3 \cup \mathcal{G}_4$, for any fixed a (resp. b) and c, the manifolds $W^u_{l\epsilon}$, $W^s_{l\epsilon}$, $W^u_{r\epsilon}$ and $W^s_{r\epsilon}$ vary monotonically as b (resp. a) varies monotonically. Specifically, when $\epsilon < 0$ for $b+\epsilon$, the manifolds $W^u_{l\epsilon}$ and $W^s_{l\epsilon}$ are situated above W^u_{l0} and W^s_{l0}, but the manifolds $W^u_{r\epsilon}$ and $W^s_{r\epsilon}$ are situated below W^u_{r0} and W^s_{r0}, respectively, as shown in* Fig. 5. *When $\epsilon < 0$ for the perturbation $a+\epsilon$, the manifolds $W^s_{l\epsilon}$ and $W^s_{r\epsilon}$ are situated above W^s_{l0} and W^s_{r0}, but the manifolds $W^u_{l\epsilon}$ and $W^u_{r\epsilon}$ are situated below W^u_{l0} and W^u_{r0}, respectively, as shown in* Fig. 6.

Please cite this article in press as: H. Chen, Y. Tang, Global dynamics of the Josephson equation in TS^1, J. Differential Equations (2020), https://doi.org/10.1016/j.jde.2020.03.048

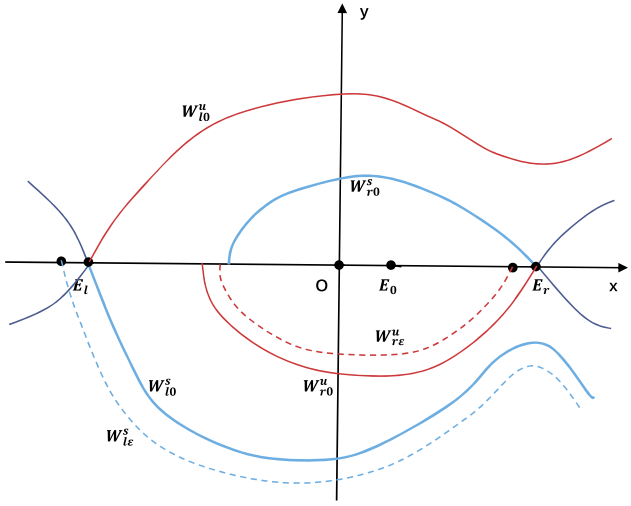

(a) $\epsilon > 0$

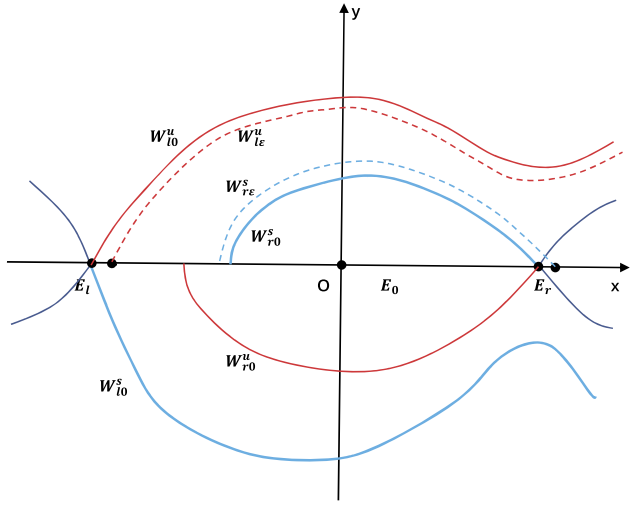

(b) $\epsilon < 0$

Fig. 6. Manifolds of saddles of system (6) under small perturbations of $a + \epsilon$ when $0 < a < 1$.

Proof. Denote the points on W^s_{l0} and $W^s_{l\epsilon}$ by $(x, y^s_0(x))$ and $(x, y^s_\epsilon(x))$, respectively, for $x \in (-\pi - \arcsin a, \delta)$ and $\delta \in (\arcsin a, \pi - \arcsin a)$. First, we consider that the manifolds $W^u_{l\epsilon}$, $W^s_{l\epsilon}$, $W^u_{r\epsilon}$ and $W^s_{r\epsilon}$ vary monotonically with respect to b. We can define the distance function $z_{1,b}(x) := y^s_\epsilon(x) - y^s_0(x)$ for all $x \in [-\pi - \arcsin a, \delta]$. Note that

$$z_{1,b}(-\pi - \arcsin a) = 0.$$

For all x in $[-\pi - \arcsin a, \delta]$, we have

Please cite this article in press as: H. Chen, Y. Tang, Global dynamics of the Josephson equation in TS^1, J. Differential Equations (2020), https://doi.org/10.1016/j.jde.2020.03.048

$$\begin{aligned} z_{1,b}(x) &= z_{1,b}(x) - z_{1,b}(-\pi - \arcsin a) \\ &= \left\{ y_\epsilon^s(\tau) - y_0^s(\tau) \right\} |_{\tau=-\pi-\arcsin a}^{\tau=x} \\ &= \int_{-\pi-\arcsin a}^{x} \left(\frac{-\sin x + a - (b + \epsilon + c\cos x) y_\epsilon^s(\tau)}{y_\epsilon^s(\tau)} \right. \\ &\quad \left. - \frac{-\sin x + a - (b + c\cos x) y_0^s(\tau)}{y_0^s(\tau)} \right) d\tau \\ &= H_1(x) + \int_{-\pi-\arcsin a}^{x} z_{1,b}(\tau) H_2(\tau) d\tau, \end{aligned} \tag{33}$$

where

$$H_1(x) := -\epsilon(x + \pi + \arcsin a), \quad H_2(x) := \frac{\sin x - a}{y_0^s(x) y_\epsilon^s(x)}.$$

It follows from (33) that

$$H_2(x) z_{1,b}(x) = H_1(x) H_2(x) + H_2(x) \int_{-\pi-\arcsin a}^{x} z_{1,b}(\tau) H_2(\tau) d\tau.$$

Letting

$$H_3(x) := \int_{-\pi-\arcsin a}^{x} z_{1,b}(\tau) H_2(\tau) d\tau,$$

we have

$$\frac{dH_3(x)}{dx} - H_2(x) H_3(x) = H_1(x) H_2(x). \tag{34}$$

Solving H_3 from (34), we obtain that

$$H_3(x) = \int_{-\pi-\arcsin a}^{x} H_1(\tau) H_2(\tau) \exp\left\{ \int_\tau^x H_2(\eta) d\eta \right\} d\tau. \tag{35}$$

Thus, by (33) and (35), we can compute that

$$\begin{aligned} z_{1,b}(x) &= H_1(x) + \int_{-\pi-\arcsin a}^{x} H_1(\tau) H_2(\tau) \exp\left\{ \int_\tau^x H_2(\eta) d\eta \right\} d\tau \\ &= H_1(-\pi - \arcsin a) \exp\left\{ \int_{-\pi-\arcsin a}^{x} H_2(\eta) d\eta \right\} + \end{aligned}$$

$$\int_{-\pi-\arcsin a}^{x} H_1'(\tau)\exp\left\{\int_{\tau}^{x} H_2(\eta)d\eta\right\}d\tau$$

$$= -\epsilon \int_{-\pi-\arcsin a}^{x} \exp\left\{\int_{\tau}^{x} H_2(\eta)d\eta\right\}d\tau$$

$$\begin{cases} <0, \text{if } \epsilon > 0, \\ >0, \text{if } \epsilon < 0, \end{cases} \tag{36}$$

which implies that $W^s_{l\epsilon}$ is situated above W^s_{l0} when $\epsilon < 0$.

Denote the points on W^u_{l0} and $W^u_{l\epsilon}$ by $(x, y^u_0(x))$ and $(x, y^u_\epsilon(x))$, respectively, for $x \in (-\pi - \arcsin a, \delta)$ and $\delta \in (\arcsin a, \pi - \arcsin a)$. We can also define the distance function $z_{2,b}(x) := y^u_\epsilon(x) - y^u_0(x)$ for all $x \in [-\pi - \arcsin a, \delta]$. Using a similar computation as for (36), we have

$$z_{2,b}(x) = -\epsilon \int_{-\pi-\arcsin a}^{x} \exp\left\{\int_{\tau}^{x} \tilde{H}_2(\eta)d\eta\right\}d\tau = \begin{cases} <0, \text{if } \epsilon > 0, \\ >0, \text{if } \epsilon < 0 \end{cases} \tag{37}$$

for all $x \in [-\pi - \arcsin a, \delta]$, where

$$\tilde{H}_2(x) := \frac{\sin x - a}{y^u_0(x) y^u_\epsilon(x)}.$$

Thus, for $0 \le a < 1$ and $\epsilon < 0$, the manifolds $W^u_{l\epsilon}$ and $W^s_{l\epsilon}$ are situated above W^u_{l0} and W^s_{l0}.

In addition, for the manifolds $W^u_{r\epsilon}$ and $W^s_{r\epsilon}$, we can also obtain that they vary monotonically with respect to b by a similar analysis as for the manifolds $W^u_{l\epsilon}$ and $W^s_{l\epsilon}$. Since the proof is similar, we omit it.

Next, we investigate the variation in the manifolds of saddles for the perturbed system $(6)|_{a\to a+\epsilon}$ when $\epsilon > 0$. For simplicity, we denote the points on W^s_{l0} and $W^s_{l\epsilon}$ by $(x, y^s_{0,a}(x))$ and $(x, y^s_{\epsilon,a}(x))$, respectively, for $x \in (-\pi - \arcsin a, \delta)$ and $\delta \in (\arcsin a, \pi - \arcsin a)$. We can define the distance function $z_{1,a}(x) := y^s_{\epsilon,a}(x) - y^s_{0,a}(x)$ for all $x \in [-\pi - \arcsin a, \delta]$. Note that $z_{1,a}(-\pi - \arcsin a) = 0$ when $\epsilon = 0$ and the equilibrium $((-\pi - \arcsin(a+\epsilon), 0)$ of perturbed system $(6)|_{a\to a+\epsilon}$ lies in a small neighborhood of the equilibrium $((-\pi - \arcsin a, 0)$ of system (6). Thus, we compute that

$$z_{1,a}(-\pi - \arcsin a)$$

$$= \frac{1}{2}(-b + c\rho - \sqrt{(c\rho - b)^2 + 4\rho})\,(\arcsin(a+\epsilon) - \arcsin a) + o(|\epsilon|) < 0, \tag{38}$$

where $\rho := \sqrt{1-(a+\epsilon)^2} > 0$ for small enough $|\epsilon|$. For all x in $[-\pi - \arcsin a, \delta]$, we have

Please cite this article in press as: H. Chen, Y. Tang, Global dynamics of the Josephson equation in TS^1, J. Differential Equations (2020), https://doi.org/10.1016/j.jde.2020.03.048

$$
\begin{aligned}
z_{1,a}(x) &= z_{1,a}(x) - z_{1,a}(-\pi - \arcsin a) + z_{1,a}(-\pi - \arcsin a) \\
&= \left(y^s_{\epsilon,a}(\tau) - y^s_{0,a}(\tau)\right)|^{\tau=x}_{\tau=-\pi-\arcsin a} + z_{1,a}(-\pi - \arcsin a) \\
&= \int_{-\pi-\arcsin a}^{x} \left(\frac{-\sin x + a + \epsilon - (b + c\cos x) y^s_{\epsilon,a}(\tau)}{y^s_{\epsilon,a}(\tau)} \right. \\
&\quad \left. - \frac{-\sin x + a - (b + c\cos x) y^s_{0,a}(\tau)}{y^s_{0,a}(\tau)} \right) d\tau + z_{1,a}(-\pi - \arcsin a) \\
&= \hat{H}_1(x) + \int_{-\pi-\arcsin a}^{x} z_{1,a}(\tau)\hat{H}_2(\tau) d\tau,
\end{aligned}
\tag{39}
$$

where

$$
\hat{H}_1(x) := \epsilon \int_{-\pi-\arcsin a}^{x} \frac{1}{y^s_{\epsilon,a}(\tau)} d\tau + z_{1,a}(-\pi - \arcsin a), \quad \hat{H}_2(x) := \frac{\sin x - a}{y^s_{0,a}(x) y^s_{\epsilon,a}(x)}.
$$

Similar to the discussion for the perturbed system $(6)|_{b\to b+\epsilon}$, we have

$$
\begin{aligned}
z_{1,a}(x) &= \hat{H}_1(x) + \int_{-\pi-\arcsin a}^{x} \hat{H}_1(\tau)\hat{H}_2(\tau) \exp\left\{ \int_{\tau}^{x} \hat{H}_2(\eta) d\eta \right\} d\tau \\
&= \hat{H}_1(-\pi - \arcsin a) \exp\left\{ \int_{-\pi-\arcsin a}^{x} \hat{H}_2(\eta) d\eta \right\} + \\
&\quad \int_{-\pi-\arcsin a}^{x} \hat{H}_1'(\tau) \exp\left\{ \int_{\tau}^{x} \hat{H}_2(\eta) d\eta \right\} d\tau \\
&= \hat{z}_{1,a}(-\pi - \arcsin a) \exp\left\{ \int_{-\pi-\arcsin a}^{x} \hat{H}_2(\eta) d\eta \right\} \\
&\quad + \epsilon \int_{-\pi-\arcsin a}^{x} \frac{1}{y^s_{\epsilon,a}(\tau)} \exp\left\{ \int_{\tau}^{x} \hat{H}_2(\eta) d\eta \right\} d\tau \\
&< 0
\end{aligned}
\tag{40}
$$

from (38) and (39). Therefore, the manifold $W^s_{l\epsilon}$ is situated below W^s_{l0}; see Fig. 6(a). By a similar investigation, we can prove that the manifold $W^u_{r\epsilon}$ is situated above W^u_{r0} when $\epsilon > 0$, the manifold $W^u_{l\epsilon}$ is situated below W^u_{l0} when $\epsilon < 0$, and the manifold $W^s_{r\epsilon}$ is situated above W^s_{r0} when $\epsilon < 0$; see Fig. 6(b). Thus, the conclusion is proven. □

Please cite this article in press as: H. Chen, Y. Tang, Global dynamics of the Josephson equation in TS^1, J. Differential Equations (2020), https://doi.org/10.1016/j.jde.2020.03.048

From Lemma 5, we can obtain the uniqueness of limit cycles but not solve the existence problem. In the following proposition, we further research the existence of limit cycles and homoclinic (or heteroclinic) orbits when $(a, b, c) \in \mathcal{G}_3$.

Proposition 8. *When $(a, b, c) \in \mathcal{G}_3$, there are three continuous functions $b = \varphi(a, c)$, $b = \psi_1(a, c)$ and $b = \psi_2(a, c)$ such that $0 < \psi_2(a, c) < \varphi(a, c) < -c\sqrt{1-a^2}$ for $0 < a < 1$, $\varphi(1, c) = 0$, $\varphi(0, c) = \psi_1(0, c) = \psi_2(0, c) > 0$ and the following statements hold:*

(a): *System (6) has one homoclinic loop that connects the right saddle $E_r = (\pi - \arcsin a, 0)$ if and only if $b = \varphi(a, c)$ for $0 < a < 1$ and one two-saddle loop if and only if $b = \varphi(0, c)$ for $a = 0$.*
(b): *System (6) has exact one limit cycle if and only if $\varphi(a, c) < b < -c\sqrt{1-a^2}$.*
(c): *System (6) has no limit cycles if and only if $0 < b \le \varphi(a, c)$.*
(d): *System (6) has an upper saddle connection if and only if $b = \psi_1(a, c)$ for $0 \le a < 1$, where ψ_1 is increasing with respect to a. There exists a unique $a^* \in (0, 1)$ such that $-c\sqrt{1-(a^*)^2} = \psi_1(a^*, c)$.*
(e): *There exists a unique $a_* \in (0, 1)$ such that system (6) has a lower saddle connection if and only if $b = \psi_2(a, c)$ for $0 \le a < a_* < 1$, where ψ_2 is decreasing with respect to a and satisfies $\psi_2(a_*, c) = 0$.*

Proof. Consider the case $b = 0$ first in parameter region $\mathcal{G}_3$. We have

$$\begin{aligned} \frac{d\Phi}{dt}|_{(12)} &= -g_a(x)F_a(x) \\ &= -c\big(\sin(x + \arcsin a) - a\big)^2 > 0 \end{aligned} \tag{41}$$

from (14), which implies that system (12) has neither limit cycles nor homoclinic loops. Note that system (12) has two saddles $\tilde{E}_R = (\pi - 2\arcsin a, F_a(\pi - 2\arcsin a))$ and $\tilde{E}_L = (-\pi - 2\arcsin a, F_a(-\pi - 2\arcsin a))$. From (13) we have

$$\Phi(\pi - 2\arcsin a, 0) = 2\sqrt{1-a^2} - a(\pi - 2\arcsin a) \tag{42}$$

and

$$\Phi(-\pi - 2\arcsin a, 0) = 2\sqrt{1-a^2} + a(\pi + 2\arcsin a). \tag{43}$$

It follows from (42) and (43) that

$$\Phi(\pi - 2\arcsin a, 0) - \Phi(-\pi - 2\arcsin a, 0) = -2a\pi \begin{cases} = 0, & \text{for } a = 0, \\ < 0, & \text{for } a > 0. \end{cases}$$

Therefore, for system (12) the unstable manifold of saddle $\tilde{E}_L$ is situated above the stable manifold of saddle $\tilde{E}_R$ in the upper half plane by (41).

With $x \to x + \arcsin a$, system (6) can be written as

$$\dot{x} = y, \qquad \dot{y} = -\sin(x + \arcsin a) + a - \big(b + c\cos(x + \arcsin a)\big)y \tag{44}$$

Please cite this article in press as: H. Chen, Y. Tang, Global dynamics of the Josephson equation in TS^1, J. Differential Equations (2020), https://doi.org/10.1016/j.jde.2020.03.048

after moving the equilibrium $E_0 = (\arcsin a, 0)$ to the origin O. Note that system (44) has three equilibria

$$E_L = (-\pi - 2\arcsin a, 0), \qquad O = (0, 0), \qquad E_R = (\pi - 2\arcsin a, 0).$$

Here, let W^u_{L0} (or W^s_{L0}) and W^u_{R0} (or W^s_{R0}) be the unstable (or stable) manifold of equilibria E_L and E_R for system (44), respectively. When $b = 0$ and $a = 0$, the equivalent system (12) of system (44) is symmetric with respect to the origin. Thus, the unstable manifold of saddle E_R is situated below stable manifold of saddle E_L of system (44) in the lower half plane, as shown in Fig. 7(a). In addition, from (13) we have

$$\lim_{a\to 1} \Phi(\pi - 2\arcsin a, 0) = 0 < \lim_{a\to 1} \Phi(-\pi - 2\arcsin a, 0) = 2\pi. \tag{45}$$

Thus, when $b = 0$ and $a \to 1$, the manifolds of the two saddles are as shown in Fig. 7(b). Actually, we can obtain that the unstable manifold of saddle E_L is situated above the stable manifold of saddle E_R of system (44) in the $y > 0$ half plane by (45). Therefore, by Lemma 7, in the $y < 0$ plane, the perturbed manifold $W^s_{L\epsilon}$ is situated below W^s_{L0}, but the perturbed manifold $W^u_{R\epsilon}$ is situated above W^u_{R0} when $a \to a + \epsilon$ and $\epsilon > 0$. Further, by Fig. 7(a)-(b) and Lemma 7, there is a unique value $a_* \in (0, 1)$ such that the unstable manifold of saddle E_R and the stable manifold of saddle E_L coincide in the lower half plane, i.e., there is a lower saddle connection between the two saddles, as shown in Fig. 7(c).

When $b = -c\sqrt{1 - a^2}$, system (44) can be written in the following form:

$$\frac{dy}{dx} = \frac{-\sin(x + \arcsin a) + a}{y} + c\sqrt{1 - a^2} - c\cos(x + \arcsin a). \tag{46}$$

With $x \to -x$, equation (46) can be changed into

$$\frac{dy}{dx} = \frac{-\sin(x - \arcsin a) - a}{y} - c\sqrt{1 - a^2} + c\cos(x - \arcsin a). \tag{47}$$

By

$$\frac{dy}{dx}|_{(46)} - \frac{dy}{dx}|_{(47)} = \frac{2a(1 - \cos x)}{y} + 2c\sqrt{1 - a^2}(1 - \cos x) \le 0 \tag{48}$$

for $y < 0$ and the comparison theorem (see [9, Chapter 2]), we have that W^s_{L0} lies below W^u_{R0} for $0 \le a < 1$ and $y < 0$. Actually, using (48), the image of the half-manifold of W^s_{L0} after the change $x \to -x$ for $x < 0$ and $y < 0$ will connect with the point $(\pi + 2\arcsin a, 0)$ and lie above the half-manifold of W^s_{L0} for $x > 0$ and $y < 0$. Thus, as $x = \pi - 2\arcsin a$, we have that W^s_{L0} lies below E_R for $0 \le a < 1$ and $y < 0$, and the relative positions of W^s_{L0} and W^u_{R0} can be obtained, i.e., W^s_{L0} is situated below W^u_{R0}. Moreover, denote the abscissa of the first intersection point of the negative x-axis and W^u_{R0} in the $y < 0$ half plane by x^3_R, and we have $-\pi - 2\arcsin a < x^3_R < 0$. When $a = 0$, system (44) is symmetric with respect to the origin, implying that W^s_{R0} is situated above W^u_{L0} in the upper half plane, as shown in Fig. 8(a) for $a = 0$. By a similar analysis as for the case of $b = 0$, we can show the relative position of the manifolds of the two saddles in Fig. 8(b) when $a \to 1$. Therefore, there is a unique value $a^* \in (0, 1)$ such that W^s_{R0} and W^u_{L0} coincide in

Please cite this article in press as: H. Chen, Y. Tang, Global dynamics of the Josephson equation in TS^1, J. Differential Equations (2020), https://doi.org/10.1016/j.jde.2020.03.048

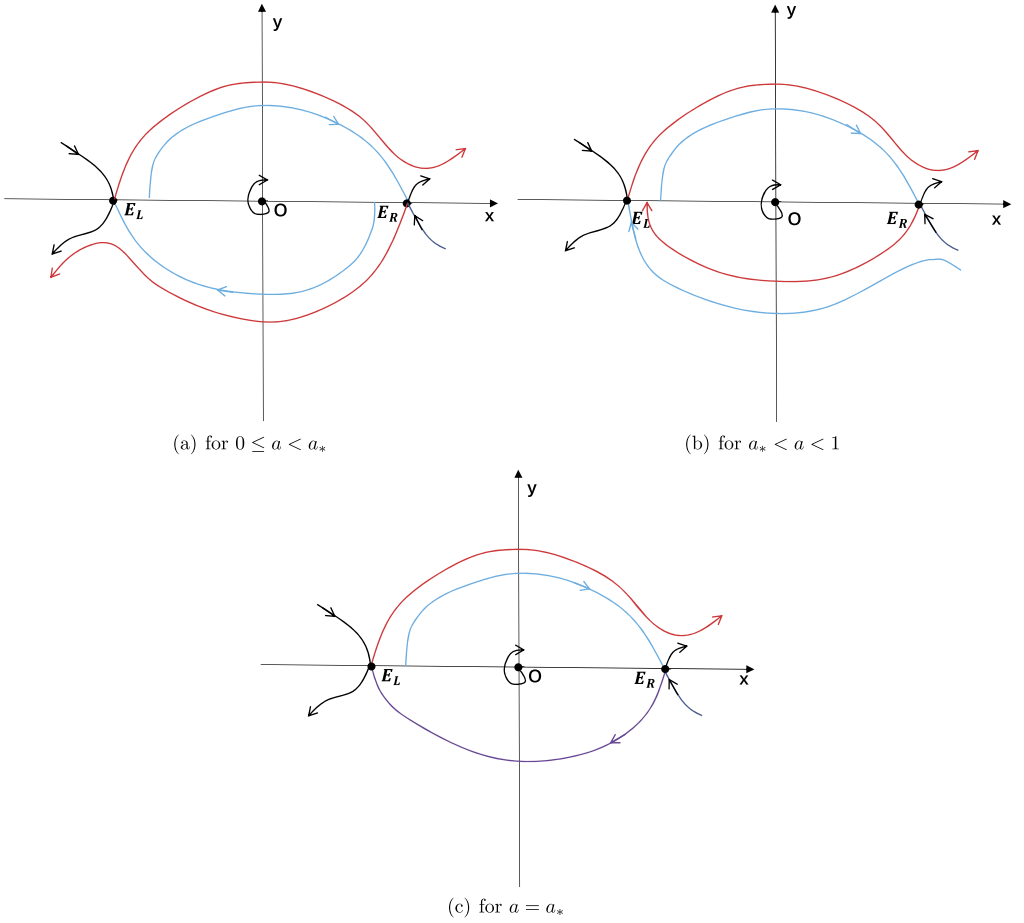

(a) for $0 \le a < a_*$ (b) for $a_* < a < 1$

(c) for $a = a_*$

Fig. 7. Manifolds of saddles of system (44) when $b = 0$.

the upper half plane by the continuity of vector fields and Lemma 7, i.e., there is an upper saddle connection between the two saddles, as shown in Fig. 8(c). Applying Lemma 7 again, there are no upper saddle connections between the two saddles when $b = -c\sqrt{1-a^2}$ and $a \neq a^*$.

By Lemma 7, Fig. 7 and Fig. 8(a, c), there is a unique function $b = \psi_1(a, c)$ such that the upper saddle connection of system (6) persists and $0 < \psi_1(a, c) \le -c\sqrt{1-a^2}$ when $0 \le a \le a^*$. Moreover, the functions $b = \psi_1(a, c)$ and $b = -c\sqrt{1-a^2}$ have a unique intersection $a = a^*$ from the above analysis for Fig. 8, i.e., $-c\sqrt{1-(a^*)^2} = \psi_1(a^*, c)$. Using the continuity of vector fields, the function $b = \psi_1(a, c)$ persists when $a^* < a \le 1$. Assume that system (6) has an upper saddle connection $b = \psi_1(a, c)$ for $(a, b, c) = (a_0, b_0, c_0)$. From Lemma 7, for $b_0 = \psi_1(a_0, c_0)$ and $\epsilon > 0$, there is a unique value $\delta > 0$ such that the upper saddle connection persists when $b_0 - \delta = \psi_1(a_0 - \epsilon, c_0)$. Therefore, ψ_1 is increasing with respect to a.

When $a = 0$, applying the symmetry of vector fields, Fig. 7(a) and Lemma 7, we can obtain a unique continuous function $b = \varphi(0, c) \in (0, -c)$ such that system (6) has a 2-saddle heteroclinic loop HE, where $\varphi(0, c) = \psi_1(0, c)$. Using a similar approach as for the upper saddle connection of system (6), we obtain the unique function $b = \psi_2(a, c)$ corresponding to the bifurcation

Please cite this article in press as: H. Chen, Y. Tang, Global dynamics of the Josephson equation in TS^1, J. Differential Equations (2020), https://doi.org/10.1016/j.jde.2020.03.048

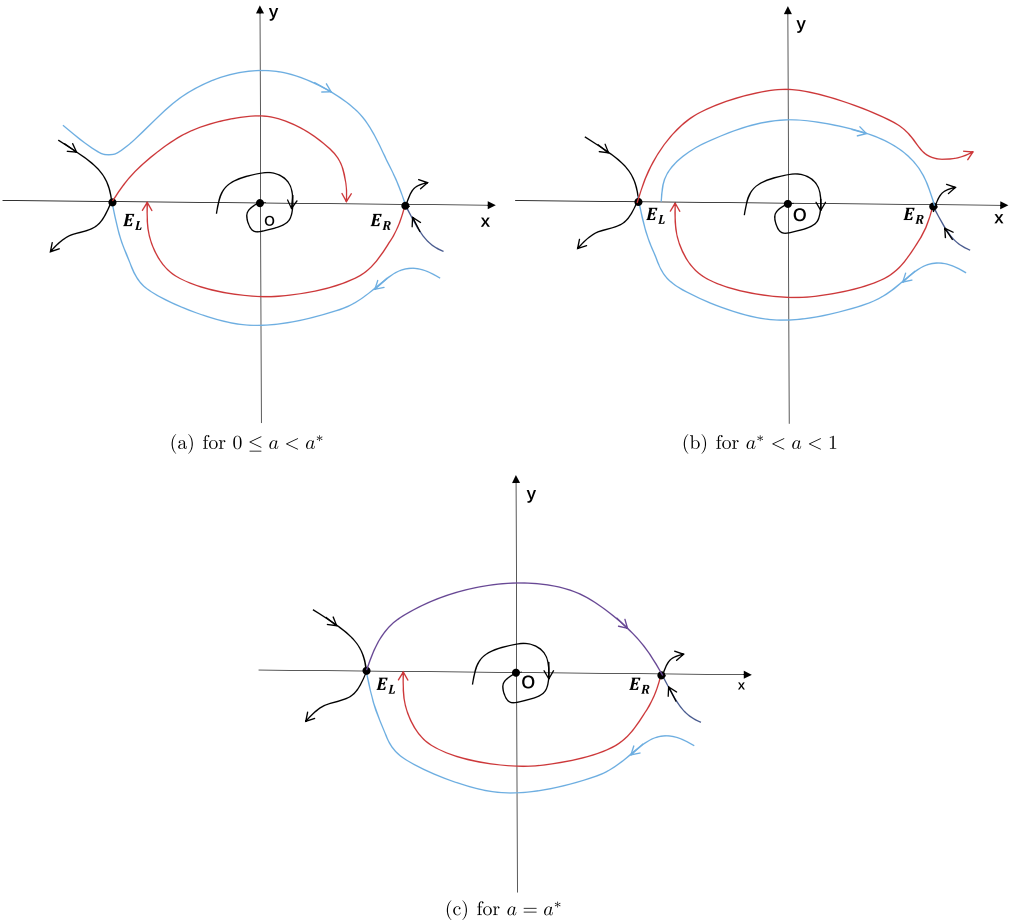

(a) for $0 \le a < a^*$ (b) for $a^* < a < 1$

(c) for $a = a^*$

Fig. 8. Manifolds of saddles of system (44) when $b = -c\sqrt{1-a^2}$.

surface of the lower saddle connection of system (6), where ψ_2 is decreasing with respect to a, $\varphi(0,c) = \psi_2(0,c)$ and $\psi_2(a_*,c) = 0$. Then, the statements **(d)** and **(e)** of this proposition are proven. Moreover, $\psi_1(a,c) > \psi_2(a,c)$ for $a > 0$ by monotonicity. In other words, system (6) has no 2-saddle heteroclinic loops for $a > 0$.

When $a_* \le a < 1$ or $a^* \le a < 1$, by Fig. 7(b, c), Fig. 8(b, c) and Lemma 7, there is a unique function $b = \varphi(a,c) \in (0, -c\sqrt{1-a^2})$ such that system (6) has a homoclinic loop that connects right saddle E_r. Obviously, $\varphi(a,c)$ should connect with Bogdanov-Takens bifurcation curve BT and 2-saddle heteroclinic loop HE. Thus, $b = \varphi(a,c)$ persists when $0 \le a \le 1$.

Consider the case $0 < a < \min\{a_*, a^*\}$. Assume that system (6) has a homoclinic loop Γ_l that connects the left saddle when $(a,b,c) = (a_0,b_0,c_0)$, as shown in Fig. 9. We can find that Γ_l lies below a stable manifold and above an unstable manifold of E_r. By Lemma 7, for fixed $(a,c) = (a_0,c_0)$, there are values b_1 and b_2 such that system (6) has an upper saddle connection for $b = b_1$ and a lower saddle connection for $b = b_2$, where $b_1 < b_0 < b_2$. In other words, we can obtain $b_1 = \psi_1(a_0,c_0) < b_2 = \psi_2(a_0,c_0)$. However, it follows from the monotonicity of $\psi_1(a,c)$ and $\psi_2(a,c)$ that $\psi_1(a_0,c_0) > \psi_2(a_0,c_0)$. Applying Lemma 7, Fig. 7(a) and Fig. 8(a), there is

Please cite this article in press as: H. Chen, Y. Tang, Global dynamics of the Josephson equation in TS^1, J. Differential Equations (2020), https://doi.org/10.1016/j.jde.2020.03.048

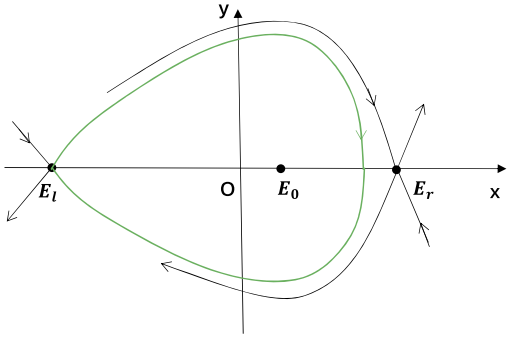

Fig. 9. Assume that system (6) has a homoclinic loop connecting E_l.

a function $b = \varphi(a, c) \in (0, -c\sqrt{1-a^2})$ such that system (6) has a homoclinic orbit that only connects with right saddle E_r.

Note that for arbitrary $b > b_*$, we have

$$\begin{aligned} &\begin{vmatrix} y - bx - c\sin(x + \arcsin a) + ac & -\sin(x + \arcsin a) + a \\ y - b_* x - c\sin(x + \arcsin a) + ac & -\sin(x + \arcsin a) + a \end{vmatrix} \\ &= (b_* - b)x\big(-\sin(x + \arcsin a) + a\big) \geq 0 \end{aligned} \tag{49}$$

when $x \in (-\pi - 2\arcsin a, \pi - 2\arcsin a)$ for system (12). Moreover, the aforementioned equality holds if and only if $x = 0$. Thus, analytic system (12) defines a family of generalized rotated vector fields for $(x, y, b) \in (-\pi - 2\arcsin a, \pi - 2\arcsin a) \times \mathbb{R} \times \mathbb{R}^+$ by Definition 3.3 in [14]. Then, the amplitude of the stable and unstable limit cycles of system (12) or its equivalent system (6) varies monotonically when b varies in a fixed direction. By the above analysis, we obtain statements **(a)-(c)** of this proposition. □

4. Proof of Theorem 1 and numerical examples

Proof of Theorem 1. Using Theorem 2, we obtain complete local properties and bifurcations of all equilibria for system (6), including saddle-node bifurcation surface SN for the three equilibria $E_l = (-\pi - \arcsin a, 0)$, $E_0 = (\arcsin a, 0)$ and $E_r = (\pi - \arcsin a, 0)$, Hopf bifurcation surface H for equilibrium E_0, local bifurcation surface of homoclinic loop HL near cusp E_r, and Bogdanov-Takens bifurcation curve BT, which is the intersection of SN, H and HL. In addition, from Proposition 8, we can present all nonlocal bifurcations, including the bifurcation surface of homoclinic loop HL, the bifurcation curve of 2-saddle heteroclinic HE, the bifurcation surfaces of upper saddle connection SC_1 and lower saddle connection SC_2 when $c < 0$. Their monotonicity with respect to the parameters and their relative positions are also obtained in this proposition. In addition, the dynamics on bifurcation surfaces and bifurcation curves have been described clearly in Theorem 2 and Proposition 8.

When $a = b = c = 0$ or $b = c = 0$ for $0 < a < 1$, system (6) is a Hamiltonian system, whose dynamics is easy to obtain, as shown in Fig. 2 (q) and (r) for dynamics in the parameter regions HEC and HLC, respectively.

When $c < 0$, from Proposition 8 and the monotonicity of functions, the function $b = \varphi(a, c)$ for the bifurcation surface of homoclinic loop HL, the function $b = \psi_1(a, c)$ for the bifurcation surface of upper saddle connection SC_1 and the function $b = \psi_2(a, c)$ for the bifurcation

Please cite this article in press as: H. Chen, Y. Tang, Global dynamics of the Josephson equation in TS^1, J. Differential Equations (2020), https://doi.org/10.1016/j.jde.2020.03.048

surface of lower saddle connection SC_2 have a unique intersection at the bifurcation curve of 2-saddle heteroclinic HE. Moreover, the functions $b = \varphi(a, c)$ and $a = 1$ and the function $b = -c\sqrt{1-a^2}$ for Hopf bifurcation have a unique intersection at Bogdanov-Takens bifurcation curve BT. The functions $b = \psi_1(a, c)$ and $a = 1$ have a unique intersection at $P_1 = (1, \psi_1(1, c))$. The function $b = \psi_1(a, c)$ and the function $b = -c\sqrt{1-a^2}$ for Hopf bifurcation have a unique intersection at $P_2 = (a^*, -c\sqrt{1-a^{*2}})$. The functions $b = \psi_2(a, c)$ and $b = 0$ have a unique intersection at $(a_*, 0)$. In addition, the dynamics on bifurcation surfaces and bifurcation curves have been clearly described in Theorem 2 and Proposition 8.

Based on the results of all bifurcation surfaces and curves, we divide the parameter space of system (6) into seven regions S_1-S_7 when $c < 0$ and three regions S_5-S_7 when $c \geq 0$, as shown in Fig. 1 for the complete bifurcation diagram. Applying Lemma 3, Lemma 4, Lemma 6 and Proposition 8, no closed orbits (including heteroclinic or homoclinic loops) exist when the parameters belong to regions S_1, S_2, S_5-S_7. Therefore, together with local dynamics, it is not difficult to obtain phase portraits when the parameters belong to these five regions. Note that system (6) has a unique stable limit cycle when $(a, b, c) \in SC_{12}$ and no limit cycles when $(a, b, c) \in SC_{11}$ because of the Hopf bifurcation at $P_2 = (a^*, -c\sqrt{1-a^{*2}})$ and the generalized rotated properties of the vector field with respect to parameter b. When $(a, b, c) \in S_3 \cup S_4$, system (6) has a unique stable limit cycle but no homoclinic loops by Lemma 5 and Proposition 8. Moreover, the relative locations of unstable (or stable) manifolds of equilibria $E_l = (-\pi - \arcsin a, 0)$ and $E_r = (\pi - \arcsin a, 0)$ can be presented by Lemma 7. Then, we have the dynamics of system (6) when $(a, b, c) \in S_3 \cup S_4$. Therefore, we can obtain all phase portraits in Fig. 2 when $c < 0$.

When $c \geq 0$, the local and nonlocal bifurcations are not as complicated as in the case of $c < 0$. There exist only the bifurcation surface of saddle-node SN and the bifurcation surface of upper saddle connection SC_1. Actually, from Theorem 2, we can obtain the bifurcation surface of saddle-node SN. When $c > 0$ and $b = 1/c$, we can obtain

$$\frac{d(y - bx - ac)}{dt}|_{(11)} = -\frac{1}{c}(y - bx - ac).$$

That is, the line $y - bx - ac = 0$ is invariant for system (11) when $b = 1/c$. Note that all three equilibria lie on the line $y - bx - ac = 0$ for $b = 1/c$. When $c > 0$ and $a = b = 0$, we can obtain the same phase portrait as in Fig. 8(a) because no limit cycles exist by Theorem 2 and Lemmas 3-4. Similarly, when $c > 0$, $b = 0$ and $a \to 1 - 0$, we can obtain the same phase portrait as in Fig. 8(b) because no limit cycles exist by Theorem 2 and Lemma 4. From Lemma 7, there is a unique value $a = a_*$ for arbitrarily fixed $c > 0$ such that system (6) has an upper saddle connection when $b = 0$. Then, there is a unique function $b = \psi_1(a, c)$ such that the upper saddle connection of system (6) persists. In addition, the bifurcation surface SC_1 of the upper saddle connection is located between the line

$$\{(a, b, c) \in \mathcal{G} : b = 1/c,\ 0 < a < 1,\ c > 0\}$$

and the line $\{(a, b, c) \in \mathcal{G} : b = 0,\ 0 < a < 1,\ c > 0\}$. When $c = 0$, the approach is similar to the case of $c > 0$. The difference is that bifurcation surface SC_1 should connect with bifurcation curve HEC according to the dynamics on this curve. □

In the following, we illustrate some theoretical results by numerical simulations.

Please cite this article in press as: H. Chen, Y. Tang, Global dynamics of the Josephson equation in TS^1, J. Differential Equations (2020), https://doi.org/10.1016/j.jde.2020.03.048

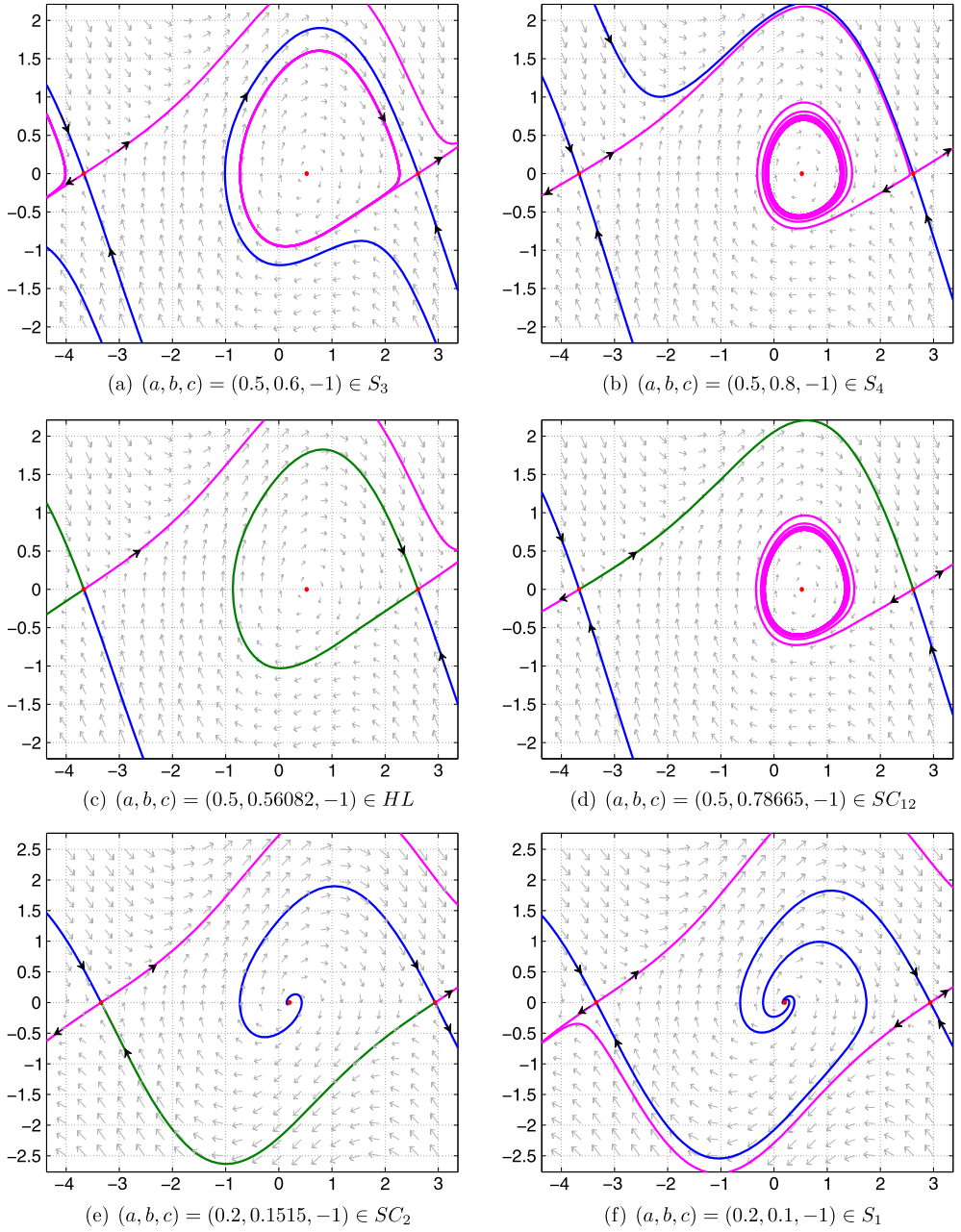

(a) $(a, b, c) = (0.5, 0.6, -1) \in S_3$ (b) $(a, b, c) = (0.5, 0.8, -1) \in S_4$

(c) $(a, b, c) = (0.5, 0.56082, -1) \in HL$ (d) $(a, b, c) = (0.5, 0.78665, -1) \in SC_{12}$

(e) $(a, b, c) = (0.2, 0.1515, -1) \in SC_2$ (f) $(a, b, c) = (0.2, 0.1, -1) \in S_1$

Fig. 10. Numerical phase portraits of (6).

Example 1. Let $(a, c) = (0.5, -1)$. When $b = 0.6, 0.8, 0.56082$ and 0.78665, we can obtain the phase portraits, as the parameters belong to the regions S_3, S_4, HL and SC_{12}, respectively, as shown in Fig. 10 (a)-(d).

Please cite this article in press as: H. Chen, Y. Tang, Global dynamics of the Josephson equation in TS^1, J. Differential Equations (2020), https://doi.org/10.1016/j.jde.2020.03.048

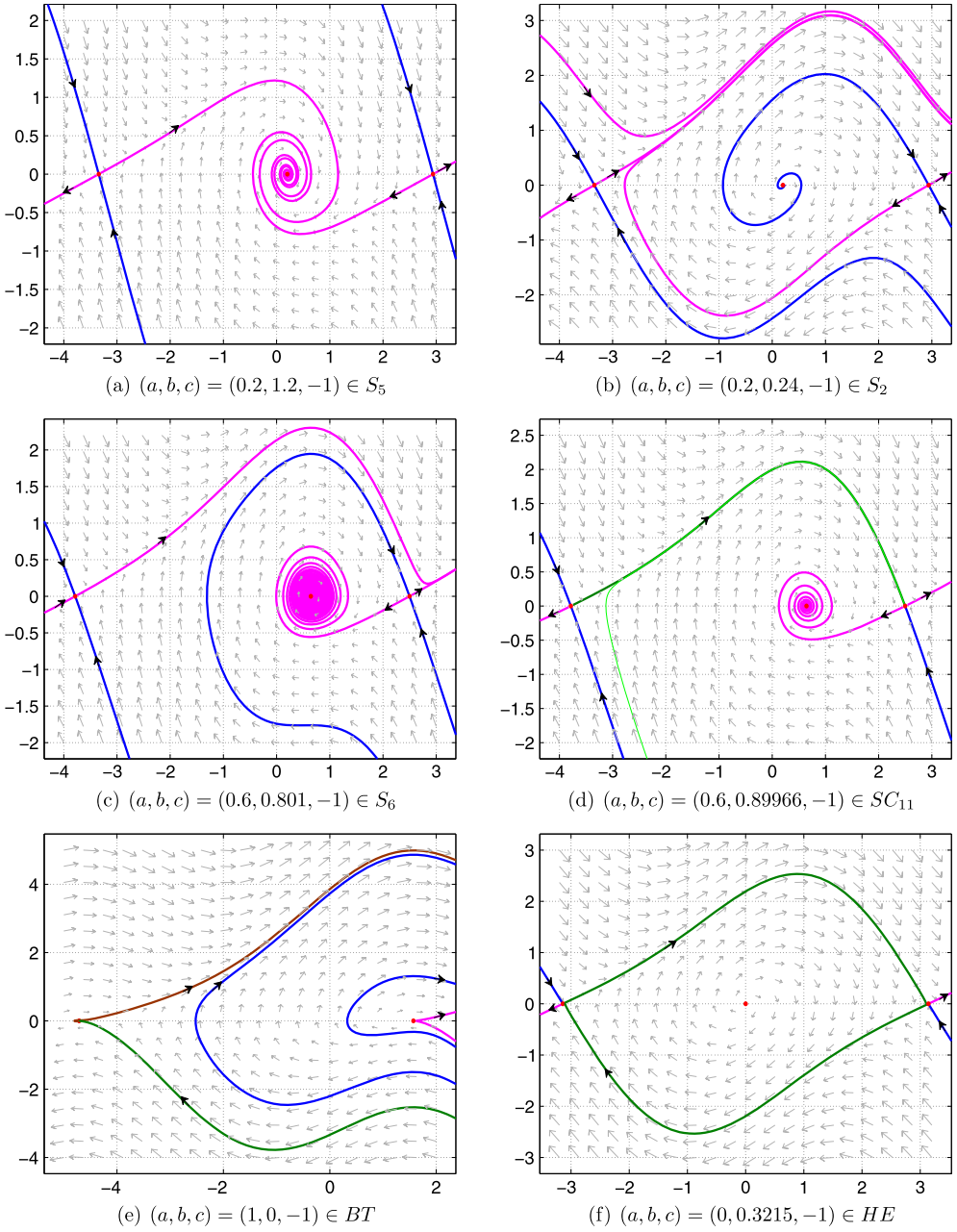

(a) $(a, b, c) = (0.2, 1.2, -1) \in S_5$ (b) $(a, b, c) = (0.2, 0.24, -1) \in S_2$

(c) $(a, b, c) = (0.6, 0.801, -1) \in S_6$ (d) $(a, b, c) = (0.6, 0.89966, -1) \in SC_{11}$

(e) $(a, b, c) = (1, 0, -1) \in BT$ (f) $(a, b, c) = (0, 0.3215, -1) \in HE$

Fig. 11. Numerical phase portraits of (6).

Example 2. Let $(a, c) = (0.2, -1)$. When $b = 0.1515, 0.1, 1.2$ and 0.24, we can obtain the phase portraits, as the parameters belong to regions SC_2, S_1, S_5 and S_2, respectively, as shown in Fig. 10 (e)-(f) and Fig. 11 (a)-(b).

Please cite this article in press as: H. Chen, Y. Tang, Global dynamics of the Josephson equation in TS^1, J. Differential Equations (2020), https://doi.org/10.1016/j.jde.2020.03.048

Example 3. Let $(a, c) = (0.6, -1)$. When $b = 0.801$ and 0.89966, we can obtain the phase portraits, as the parameters belong to regions S_6 and SC_{11} respectively, as shown in Fig. 11 (c)-(d).

Example 4. When $(a, b, c) = (1, 0, -1)$ and $(a, b, c) = (0, 0.3215, -1)$, we can obtain the phase portraits, as the parameters belong to regions BT and HE respectively, as shown in Fig. 11 (e)-(f).

Acknowledgments

The first author is supported by the National Natural Science Foundation of China (No. 11801079). The second author is supported by the National Natural Science Foundation of China (No. 11931016, 11871041, 11431008), and the International Cooperation Fund of Ministry of Science and Technology of China.

References

[1] H. Chen, X. Chen, Dynamical analysis of a cubic Liénard system with global parameters, Nonlinearity 28 (2015) 3535–3562.
[2] S.-N. Chow, C. Li, D. Wang, Normal Forms and Bifurcation of Planar Vector Fields, Cambridge Press, 1994.
[3] R.N. D'Heedene, For all real μ, $\ddot{x} + \mu \sin \dot{x} + x = 0$ has an infinite number of limit cycles, J. Differ. Equ. 5 (1969) 566–571.
[4] F. Dumortier, C. Rousseau, Cubic Liénard equations with linear damping, Nonlinearity 3 (1990) 1015–1039.
[5] H.J. Eckuteiler, Nonlinear Differential Equations of the van der Pol Type with a Variety of Periodic Solutions, Studies in Nonlinear Vibration Theory, Institute of Mathematics and Mechanics, New York University, 1946.
[6] A. Gasull, A. Geyer, F. Mañosas, On the number of limit cycles for perturbed pendulum equations, J. Differ. Equ. 261 (2016) 2141–2167.
[7] A. Gasull, J. Giné, C. Valls, Center problem for trigonometric Liénard systems, J. Differ. Equ. 263 (2017) 3928–3942.
[8] A. Gasull, J. Giné, C. Valls, Highest weak focus order for trigonometric Liénard equations, Ann. Mat. Pura Appl. (2020), in press, https://doi.org/10.1007/s10231-019-00936-8.
[9] J. Hale, Ordinary Differential Equations, Krieger Publishing Company, 1980.
[10] H. Hochstadt, B. Stephan, On the limit cycles of $\ddot{x} + \mu \sin \dot{x} + x = 0$, Arch. Ration. Mech. Anal. 23 (1967) 369–379.
[11] R.L. Kautz, On a proposed Josephson effect voltage standard at zero current bias, Appl. Phys. Lett. 36 (1980) 386–388.
[12] J.A. Sanders, R. Cushman, Limit cycles in the Josephson equations, SIAM J. Math. Anal. 17 (1986) 495–511.
[13] R.J. Soulen, R.P. Giffard, Impedance and noise of an rf-biased RSQUID operated in a nonhysteretic regime, Appl. Phys. Lett. 32 (1978) 770.
[14] Z. Zhang, T. Ding, W. Huang, Z. Dong, Qualitative Theory of Differential Equations, Transl. Math. Monogr., Amer. Math. Soc., Providence, RI, 1992.

Please cite this article in press as: H. Chen, Y. Tang, Global dynamics of the Josephson equation in TS^1, J. Differential Equations (2020), https://doi.org/10.1016/j.jde.2020.03.048